Name: Kendal Grubb

Class: GEOL 394

Advisors: Dr. Mong-Han Huang and Dr. Nicholas Schmerr

Date: 27 April, 2021

Comparing Changes in Meltwater Accumulation to Glacial Flow in Northwest Greenland

Abstract

Recently, a few subglacial lakes have been discovered underneath the Greenland Ice Sheet, one of them located about 70 kilometers northeast of the town of Qaanaaq. Because of rapid climate change, much of the area has melted, and subglacial lakes formed from surface crevasses that allowed meltwater to flow down towards bedrock and accumulate in valleys. At the same time, there was an extensive amount of meltwater both along the surface of the ice sheet and around bedrock flowing towards the sea. Since the ice melted away and flowed away, significant mass loss and lowered glacier surface elevation occurred, but not necessarily significant acceleration of surface glacial flow. Through the Gravity Recover and Climate Experiment (GRACE) satellites, gravity loss accelerated over the summer of 2015 in comparison to other recent years, indicating major mass loss. 2015 was also subject to a near record-breaking warm summer, with the average temperature of the northwest coast saw a 1.5°C. Because of the abnormal temperatures and mass loss, GRACE was used to analyze surges in in mass loss near the local subglacial lake. However, the data was not effective in demonstrating changes in meltwater displacement. For additional information on supraglacial flow, focus was moved to analyzing supraglacial lakes. Using USGS Landsat 8 Surface Reflectance Tier 1 maps through the Google Earth Engine, multiple supraglacial lakes can be observed. In 2015, there were three relatively large supraglacial lakes near the lake near Qaanaaq. These supraglacial lakes were frozen over during the winter of most years. Despite 2016 and 2019 having the two warmest summers ever recorded by the National Oceanic and Atmospheric Association (NOAA), they had very little sign, if any, that summer meltwater was present at the same location. The only other year, other than 2015, that all three lakes showed any meltwater was 2020, a relatively cool year in comparison to 2016 and 2019 in northwest Greenland. Based on GRACE data, the ice sheet near the lake lost the most mass in 2020, possibly indicating the resurgence of meltwater accumulation in these depressions. 2015 did not have significant mass loss acceleration in comparison to 2019 and 2020. Based on SAR data released by the National Ice and Snow Data Center (NISDC), ice velocity differences between 2015/2016 and 2017/2018 had miniscule changes. Without any correlation to accelerated mass loss and ice velocity, there is not an obvious explanation through glacial movement on why the lakes had such a large amount of meltwater in 2015.

Introduction

Over the past 20 years, the Greenland Ice Sheet has been subjected to extensive melting due to rising temperatures, particularly along the coastal areas. In some basins, crevasses form, allowing meltwater to seep beneath the surface and accumulate as subglacial lakes, usually hundreds of meters down (Willis et al., 2015). In 2018, Dr. Nicholas Schmerr led a team to an area just northeast of Qaanaaq, Greenland, in order to study one of these lakes. From a preliminary campaign using a GPS station deployed on the glacier near Qaanaaq in the Summer of 2018, there was both a horizontal displacement within nine weeks and evidence of a subglacial lake (Moy, 2019). In addition, meltwater can also form in depression on the glacial surface, forming what is called a supraglacial lake. There are several lakes scattered across the Greenland Ice Sheet, mostly near the coast, that freeze over during winter. Both subglacial and supraglacial lakes located in Greenland and Antarctica have been analyzed for various reasons including tracking glacial flow momentum and measuring heat latency (Bowling et al., 2019)(Sundal et al., 2009)(Willis et al., 2015). Since the decrease water discharged into the ocean that is remaining along the ice sheet, which impacts glacial force, outlet glacier mass and other values, it is important to understand the relevance of meltwater accumulation to other glacial flow mechanics. The plan originally was to use satellite-based remote sensing measurements to further quantify changes in mass, ice thickness, and surface flow in time, particularly during summer 2015, which had a major melting event. Accounting for supraglacial lake appearances, I hypothesized that the amount of meltwater accumulated in glacial lakes is directly correlated to the changes in glacial flow, primarily mass loss, displacement, and ice thickness. The area focused on was around 80 kilometer radius of the hypothesized subglacial lake in northwest Greenland. The remote sensing data that was used were: (1) gravity loss and mass change due to surface ice lowering from GRACE and CryoSAT-2 datasets, (2) imagery of supraglacial lakes and crevasses from Landsat 8, (3) glacial flow rates from Sentinel-1 SAR, and (4) weather patterns provided by Giovanni (NASA) and a National Oceanic and Atmosphere Association (NOAA) weather station.

Subglacial Lakes

Over the past few years, scientists have used radar and seismology to discover dozens of subglacial lakes across the Greenland and Antarctic Ice Sheets (Bowling et al., 2019; Palmer et al., 2015). Formed on top of bedrock hundreds of meters below the ice surface, the exact volume of these lakes is unknown, but potentially are made up of millions of cubic meters of glacial meltwater (Willis et al., 2015). These lakes can form by at least three processes, demonstrated in Figure 1 and 2. The first is meltwater flowing down from the ice surface (Willis et al., 2015). Caused by shear stress from the ice flowing slightly different directions, refreezing or other types of weathering, crevasses can form within basins whose depth can reach bedrock (Bowling et al., 2019; Willis et al., 2015). Ice that has melted on the surface flows down into the crevasses and accumulates along the bedrock (Bowling at al., 2019; Willis et al., 2015). Given that ice is less dense than liquid water, the ice rises, allowing more room for the water to accumulate (Willis et al., 2015). The second possible process is similar, except meltwater flows from further inland and accumulates in one area (Bowling, et al., 2019). This mechanism is predominantly found in Antarctica and rarely in Greenland. (Bowling et al., 2019; Palmer et al., 2015). However, given

that water flows downhill, the meltwater behaves in a similar fashion to runoff, flowing into the ocean over the bedrock (Bowling et al., 2019; Howat et al., 2015; Willis et al., 2015). The final process is that subsurface ice melts within areas of enhanced geothermal heat flux (Bowling et al., 2019). The water accumulates in valleys in bedrock within depressions (Bowling et al., 2019). Sometimes, multiple factors cause a lake to expand or simply be recharged. For example, ice melted by geothermal heat can be recharged by surface meltwater flowing downward through crevasses. Unfortunately, because the lakes are buried under several thousand meters of ice, it is difficult to distinguish between ice and liquid water, making the lakes more difficult to locate. No matter the cause, the high pressure at great depths often increases shear stress, expanding the cavity where the meltwater resides and increasing the overall volume of the lake.

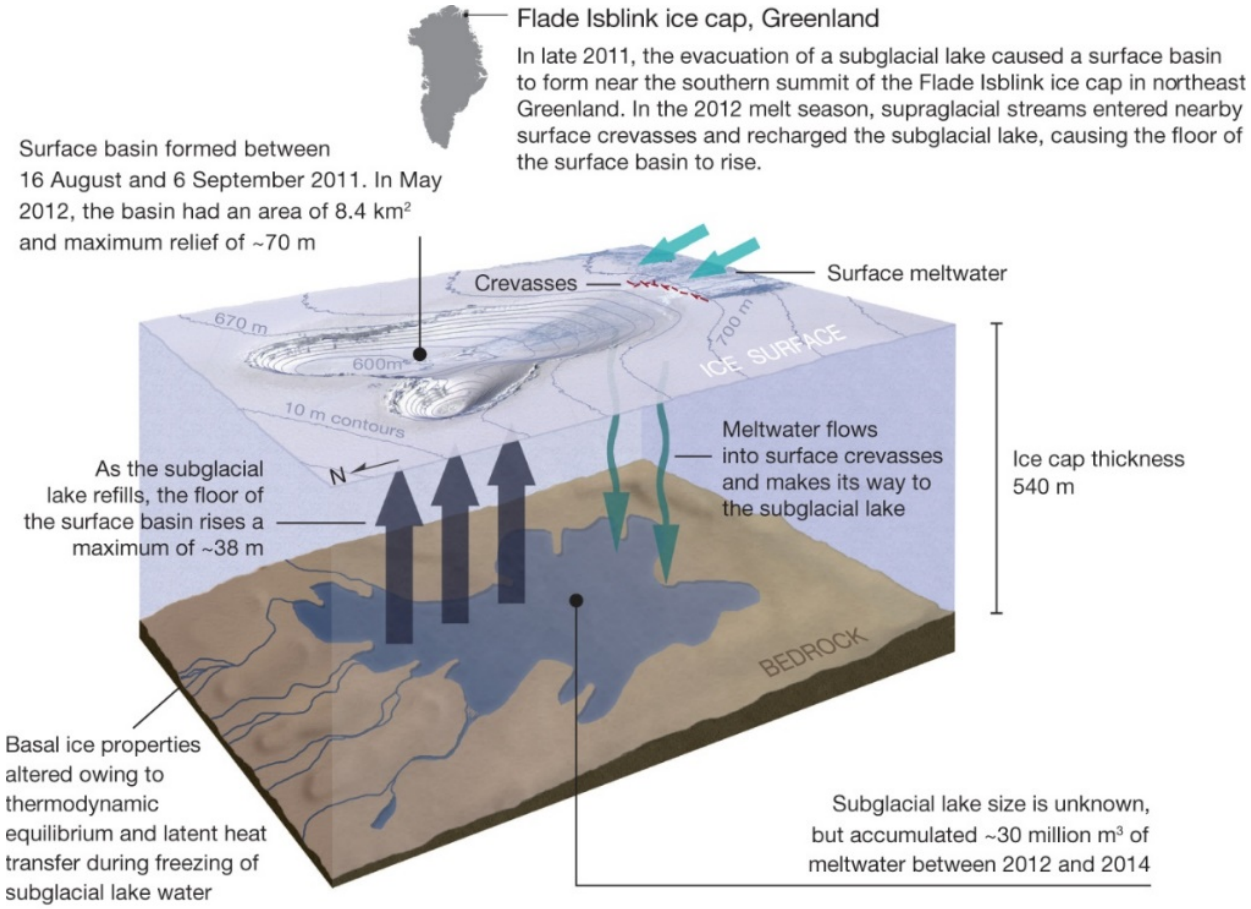

Figure 1:
3D Diagram of a subglacial lake recharged by surface meltwater flowing through crevasses within basins (Willis et al., 2015)

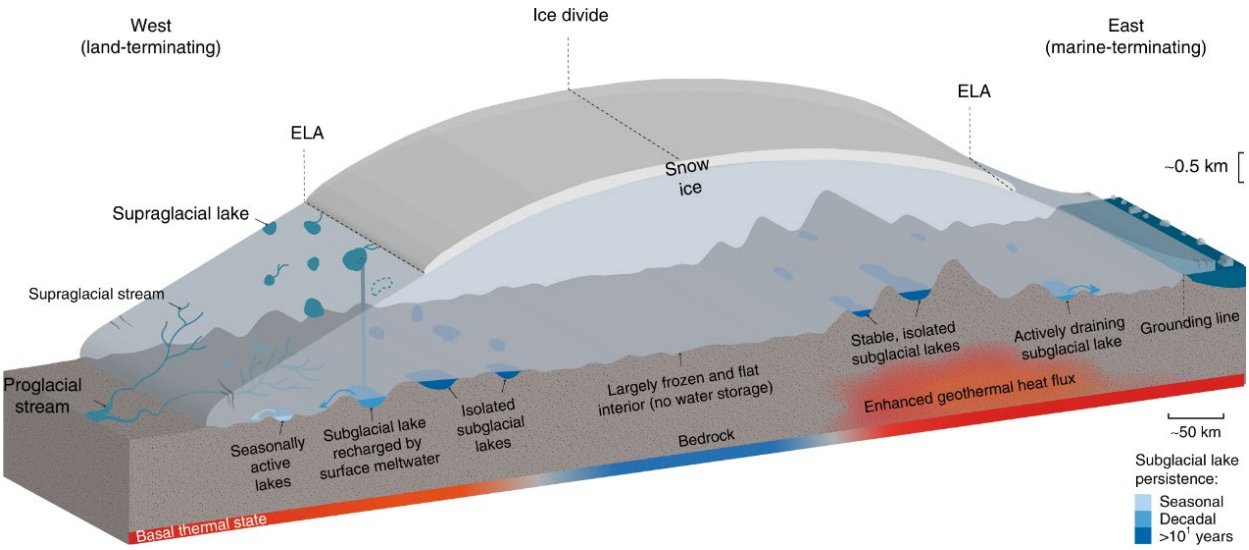

Figure 2: 3D schematic of the generic impact of geothermal heat on subglacial and supraglacial lakes (Bowling et al., 2019)

Supraglacial Lakes

Similar to their subglacial counterparts, almost all supraglacial lakes are formed when meltwater and/or precipitation runoff amasses in glacial depressions (Sundal et al., 2009). The other method is that ice in a small area with a lower albedo surrounded by an area with a higher albedo will melt while the nearby ice remains a solid (Lüthje et al., 2006). If there is a low slope, the water is trapped due to gravity. Unlike subglacial lakes where the temperature is constant, supraglacial lakes are subjected to changing temperatures, and therefore, freeze over during winter months, requiring water recharge every melting season in order for it to remain a lake. These lakes are much easier to analyze as they can be detected by both satellite imagery and field measurements. However, they are impacted by changes in weather and landscape, therefore, annual predictions are difficult to make.

Gravity Anomalies

A gravity anomaly is simply defined as the difference between a measurement of gravity and the theoretical measurement (Hackney & Featherstone, 2003). In order to quantify gravity, there are three major factors to calculate.

The first is called the latitude correction, which is the measure of the difference in gravity based on a given latitude. The equation that describes this correction is called the Somigliana- Pizetti equation, and can be found as:

$$\gamma = \gamma_a \frac{k sin^2(\varphi)+1}{\sqrt{1-e^2 sin^2(\varphi)}}$$ Equation 1: (Hackney & Featherstone, 2003)

where γ_a is the normal gravity at the equator, k is the normal gravity constant, e is the first numerical eccentricity and φ is the geodetic latitude of the ellipsoid.

The second factor is the free-air reduction, which corrects the observed gravity not made on the surface of vertical datum. It can be calculated by using the equation:

$$\delta g_F = 2\bar{g}R(h - N)$$ Equation 2: (Featherstone & Dentith,1997)

where $\bar{g}$ is the average gravity on a spheroid, R is the radius of the Earth, h is the height of a GPS signal above the surface and N is the difference between the Earth as an ellipsoid and the Earth as a geoid caused by gravity.

The third factor is the Bouguer gravity reduction, which integrates the gravitational effect on the height and/or depth of the topography. With the same variables as the free-air reduction equation, the magnitude of this anomaly can be calculated by using the equation:

$$\delta g_B = 2\pi G\rho(h - N)$$ Equation 3: (Featherstone & Dentith, 1997)

where G is Newton's Gravitational constant and ρ is the mean topographic density.

In order to calculate the sum of the anomalies, the corrections are combined into one equation:

$$\Delta g_B = g_s - \gamma + \delta g_F - \delta g_B$$ Equation 4: (Featherstone & Dentith, 1997)

where g_s is the surface gravity measurement in a given location. Using this equation, scientists can determine the gravity anomalies by measuring the needed variables.

Due to the quicker and global response, the more commonly used method to determine gravity anomalies is the use of the Gravity Recovery and Climate Experiment (GRACE). Launched in 2002, two satellites circle the planet under a polar orbit and constantly measure their position through GPS and relative to both stars and distance to each other (NASA Facts, 2003). This way, small changes in the distance between the two satellites demonstrate an anomaly in the gravity field originating from the surface of the planet, which Figure 3 displays. National Aeronautics and Space Administration (NASA) publishes acceleration and localized Water Equivalent Thickness (WET), or the gravity lost or gained under a certain thickness of water on the surface that has been determined by GRACE (NASA Facts, 2003). If there is a decrease in WET, there is a decrease in ice mass in the measured area. Given that GRACE uses precise technology and calculations, it is less prone to error, having an accuracy of 1.5 centimeters (Jiang et al., 2014), and is widely used by scientists to analyze the changes in gravity.

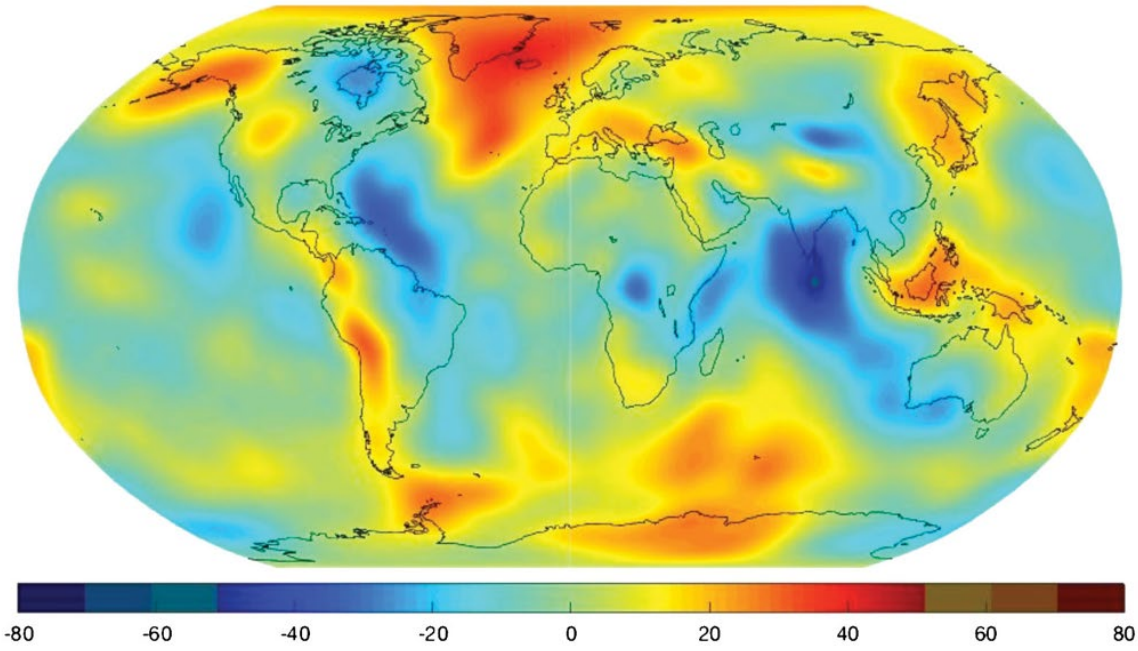

Figure 3. GRACE Gravity Model 05 displays the gravity anomalies on Earth's surface, measured in mGal, a unit of acceleration. Factors that can impact gravity anomalies include glaciers/ice caps, mountains, ocean currents, sea level change, sediment deposits and tectonics (Reis et al., 2016).

Climate Impact on Greenland

Since the launch of the GRACE satellite in 2002, scientists have determined that Greenland has lost an average of 265 ± 59 gigatons/year of ice with an average acceleration of 29.7±1.3 gigatons/years^2, resulting from major melting events due to higher surface temperatures (Velicogna et al., 2014). Throughout the GRACE mission, there were several summers that hosted high enough temperatures to have major melting events. For example, the Flade Isbink Ice Cap, a glacier located on a peninsula in northeast Greenland, had experienced sudden uplift in 2012 due to excessive subglacial meltwater presence, as demonstrated in Figure 4 (Willis et al., 2015).

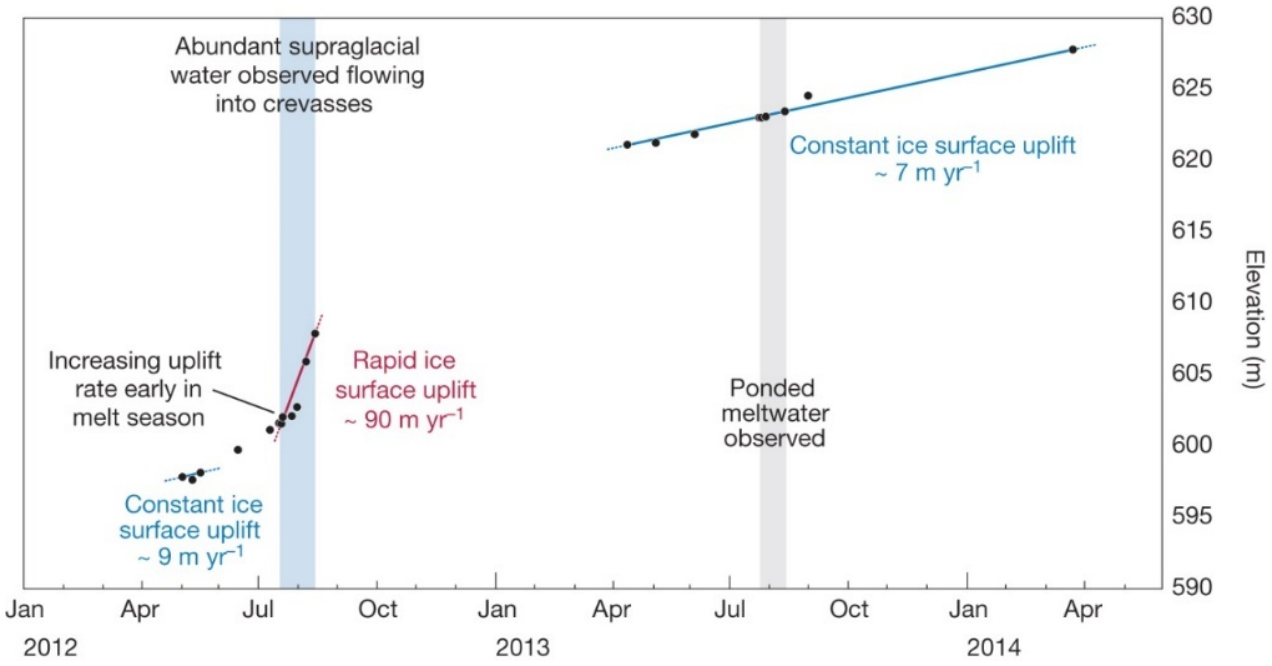

Figure 4: Graph of the uplift at the Flade Isbink Ice Cap in northeast Greenland (Willis et al., 2015).

Since melting events are dependent on air temperature, it's important to compare the ecord can vary frequently between the various melting seasons.

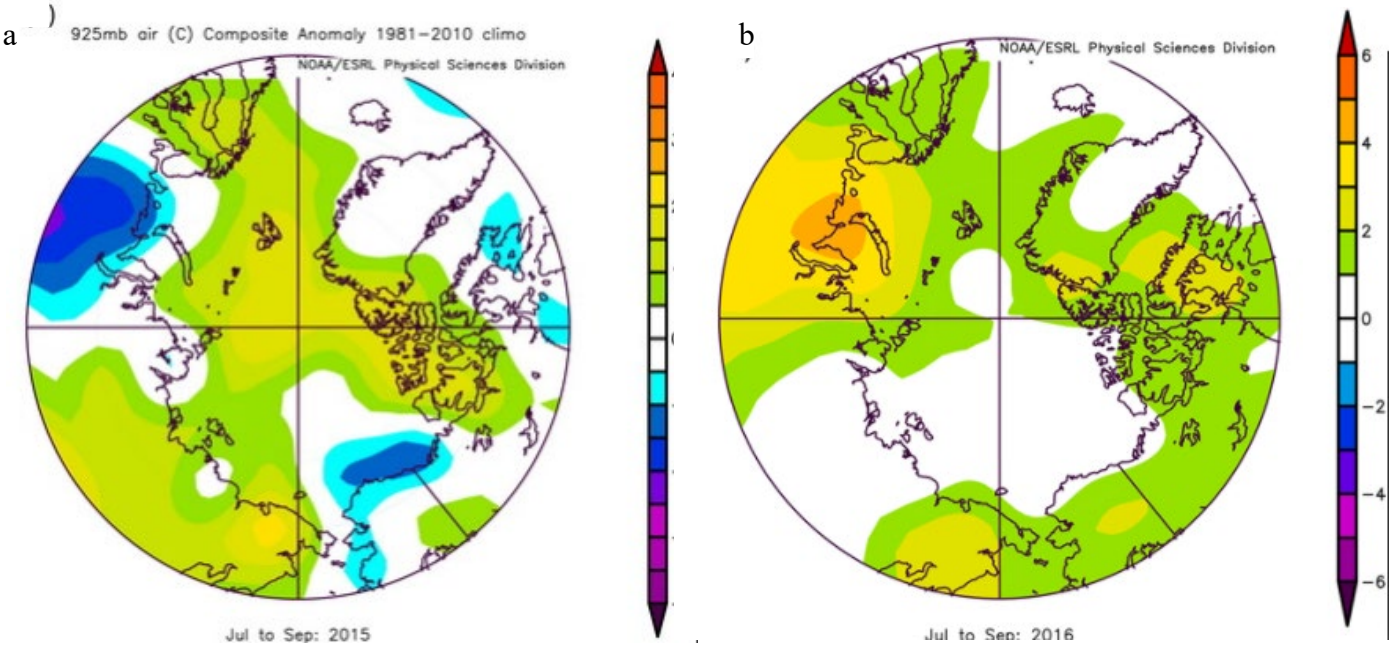

Figure 5: Differences in temperature (in Celsius) between the averages from 1981-2010 from July to September. a. 2015 (Jeffries et al., 2015) b. 2016 (Ritcher-Menge et al., 2016)

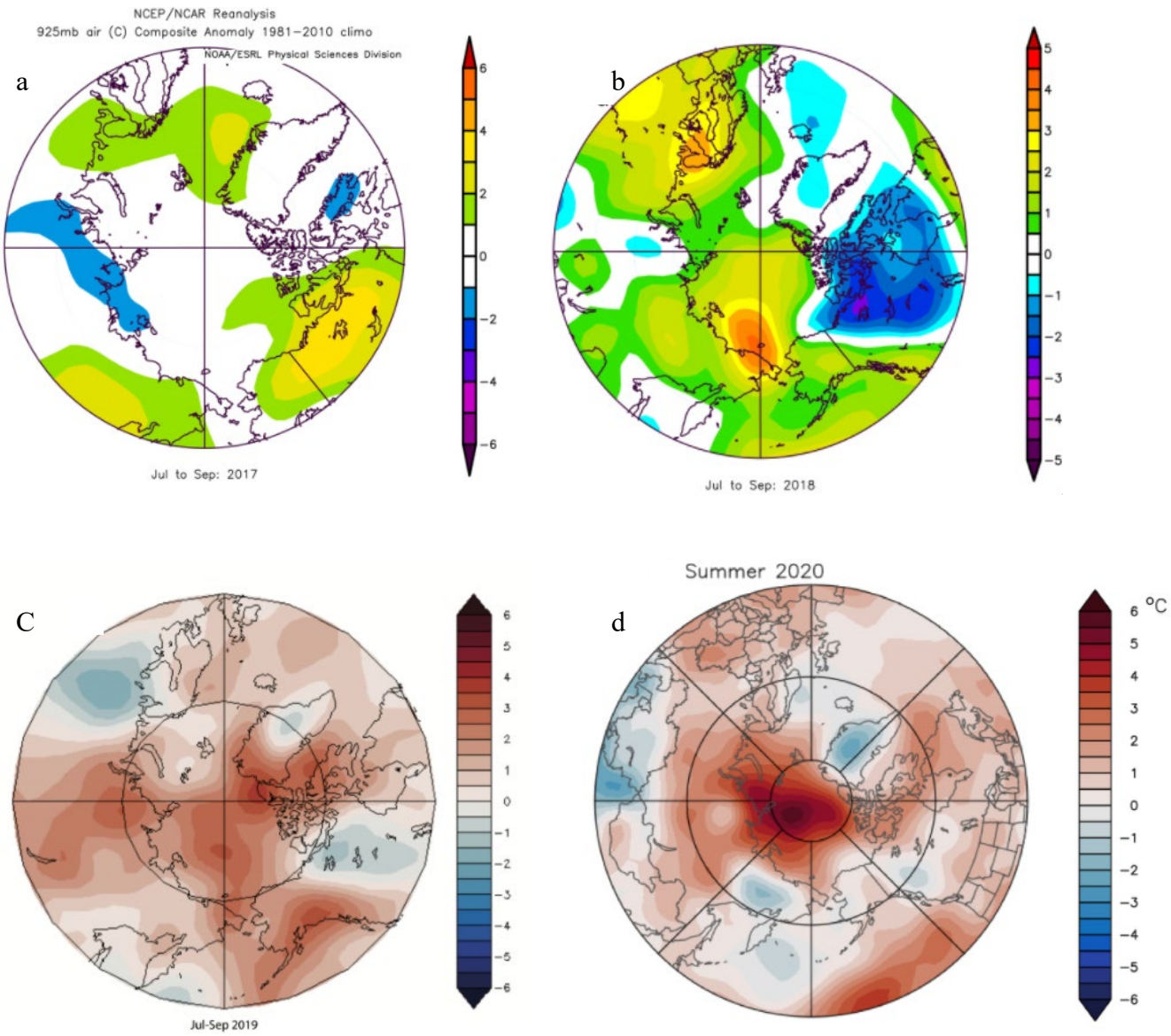

Figure 6: Temperature differences in Celsius between the averages from 1981-2010 from July to September. a. 2017 (Ritcher-Menge et al., 2017) b. 2018 (Osborne et al., 2018) c. 2019 (Ritcher-Menge et al., 2019) d. 2020 (Thoman et al., 2020)

Figures 5 and 6 indicate major heating events in northwest Greenland during the summers of 2015, 2016 and 2019, while 2017 and 2018 were average. The summer of 2020 had different numbers across the Arctic, although the ice sheet appears to be cooler than average while the ocean is still warmer.

In order to confirm that there were heating events, average temperatures were calculated. NASA currently hosts Giovanni, an online display of physical parameters, most notably atmospheric temperatures in a pre-selected area (Acker, 2007). For the purpose of calculating accurate representations of temperatures in the study area, monthly summaries were downloaded and observed.

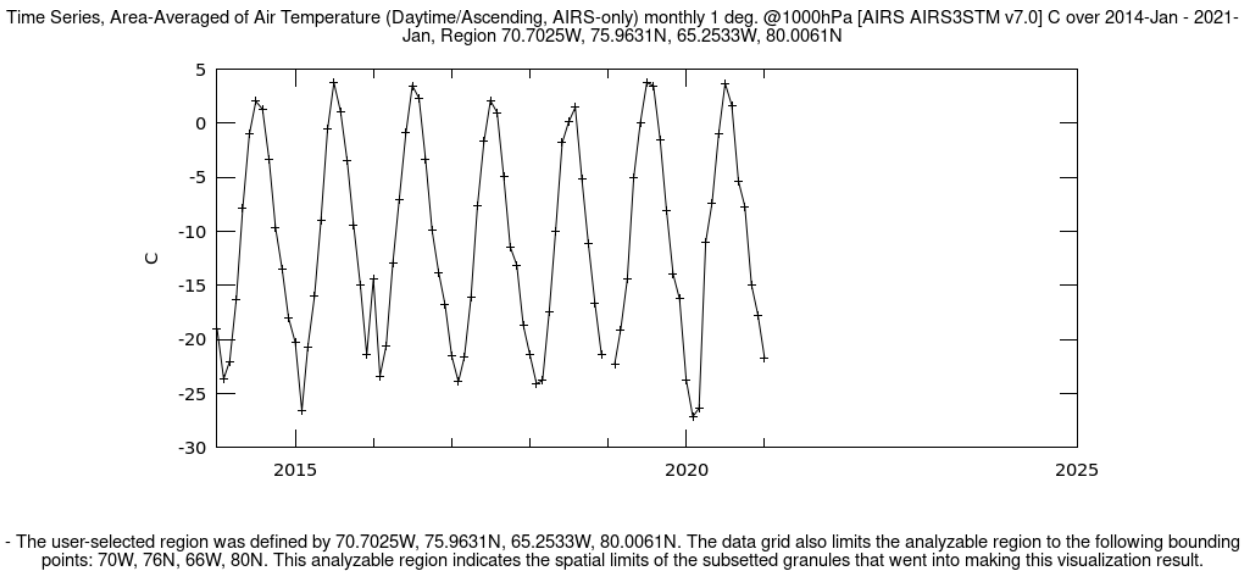

Figure 7: The Giovanni atmospheric temperature data from the study area (Acker, 2007).

Based on Figure 7, the years of 2015, 2016, 2019 and 2020 had higher temperatures in comparison to 2014, 2017 and 2018. 2020 appears to be slightly different than the maps, possibly because the area in Figure 7 covered not just landmasses but oceanic temperatures as well.

Because Giovanni was missing several daily reports, other sources were examined. Additional temperature data was provided by the closest operating NOAA weather station to the study area in Pitukiff, Greenland, approximately 175 kilometers south, shown on Figure 8. Daily reports and monthly summaries from 2014-2020 were given by NOAA Climate Data Center.

For the Pituffik weather station, several monthly temperature averages were missing from the record, with only maximum temperatures being consistently reported. Daily summaries were much more detailed but more difficult read on a graph. Since putting all seven years on the graph made it too difficult to read, Figures 9 and 10 were made of the years matching GRACE data that will be discussed later in this paper.

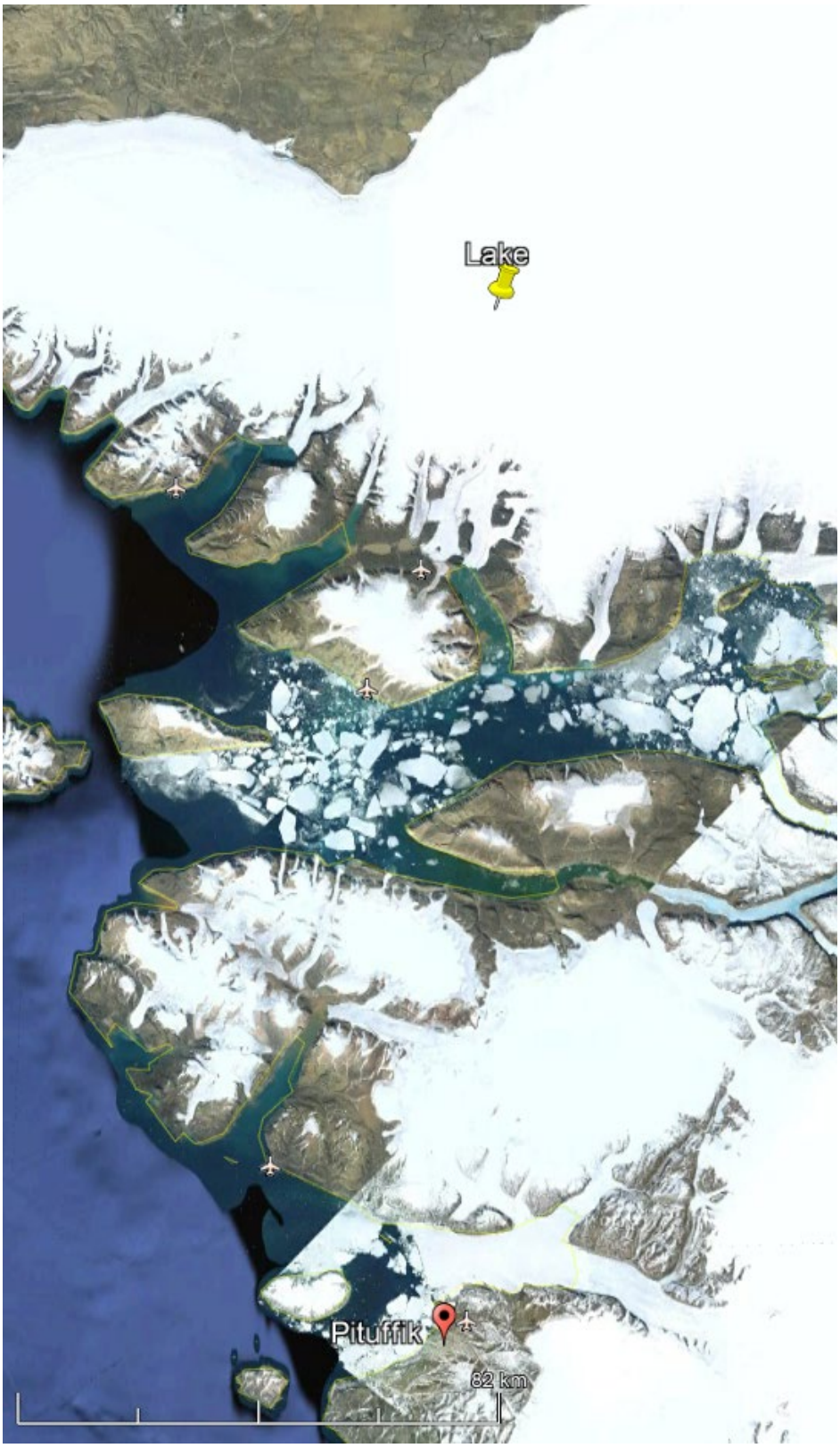

Figure 8: Hypothesized Lake Location comparison to the Pitukiff Weather Station. Image from Google Earth.

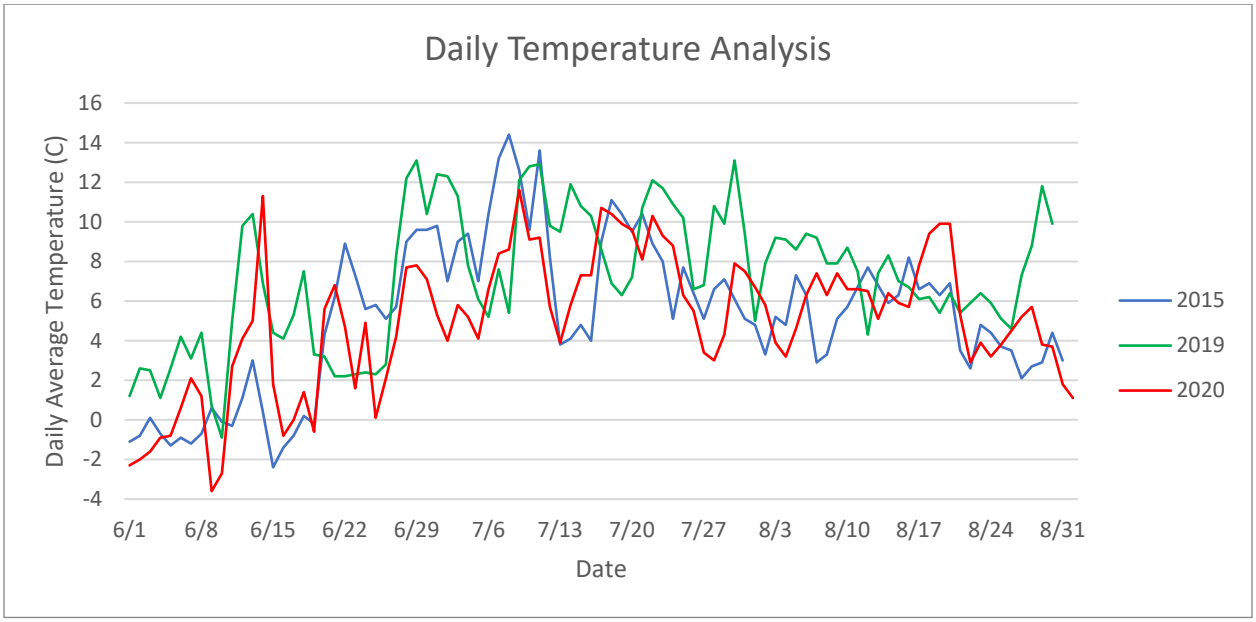

Figure 9: Daily temperatures for summer months during 2015, 2019 and 2020. For consistency's sake, only summer months are included, despite the melting season beginning in early June and often continuing in mid-September some years.

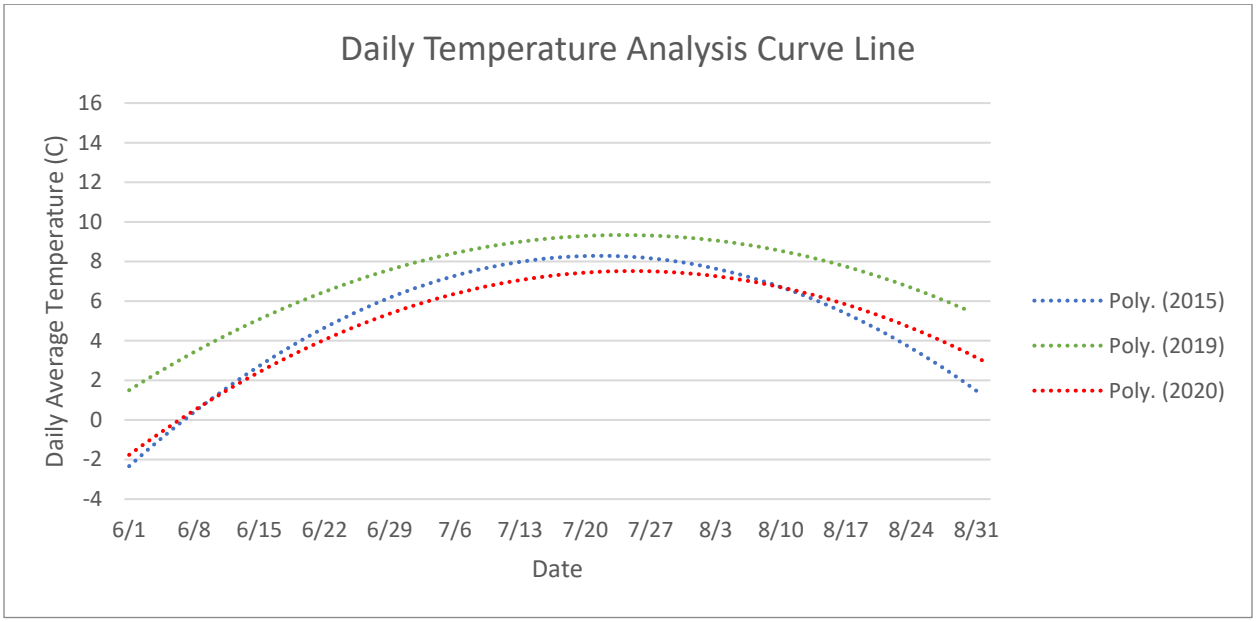

Figure 10: 2nd-Order Polynomial trendlines calculated from daily temperatures analysis using equations from Table 1. From these lines, 2019 was a particularly warm summer even in comparison to 2015 and 2020.

Table 1: Trendline Equations for Pitukiff Weather Station Temperatures

Year	Equation	Coefficient of Determination
2015	$y = -.0042x^2 + 351.37x - 7x10^6$	.5646
2019	$y = -.0028x^2 + 234.95x - 5x10^6$	.3859
2020	$y = -.0032x^2 + 269.06x - 6x10^6$	.5203

Based on the data provided by NOAA Climate Center, precipitation is often rare in the summer, particularly during warmer seasons. Monthly total precipitation is usually no more than 2 centimeters. It should have no impact of meltwater accumulation in supraglacial lakes. From a temperature standpoint alone, it appears that 2019 should have the most amount of meltwater, and therefore, the largest supraglacial lakes. This information may not be completely accurate as the weather station is still over 175 kilometers south of study area.

Lake Locations

There are over two dozen known subglacial lakes in Greenland alone, most along the coastline and/or ice divides (Bowling et al., 2019). This thesis will focus on the 80-kilometer radius around one located at 78.057396° N, 68.466962° W, approximately 69 kilometers northeast of the town of Qaanaaq.

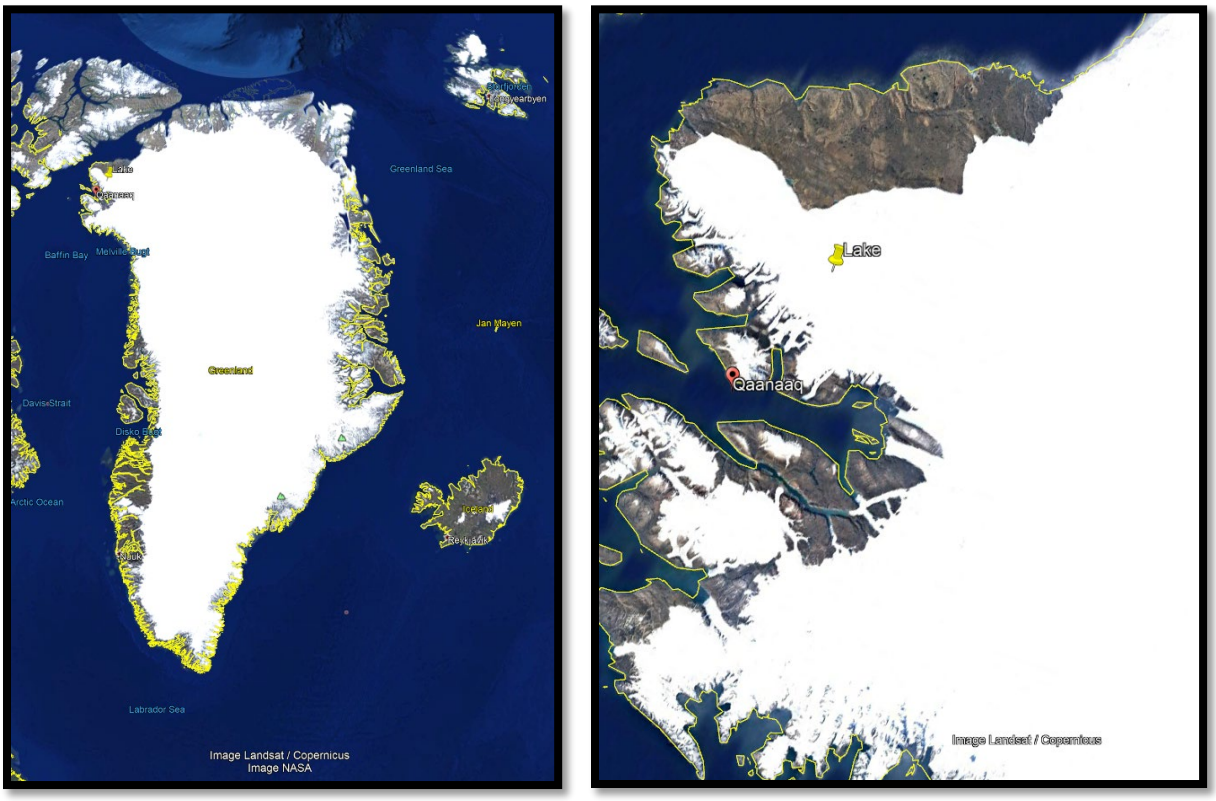

Figure 11: Subglacial lake location. Image from Google Earth

USGS Landsat 8 Reflectance Tier 1 was used to capture accurate imagery for various supraglacial lakes in the nearby area. This satellite had with 30-meter resolution to view the surface over the course of time (Acharya & Yang, 2015). After analyzing the 2015 Landsat 8 data, three lakes were found on the ice sheet within a 100-kilometer radius of the proposed sub-glacial lake, excluding those that appeared to be on outlet glaciers where the slope and ice velocity would be much higher (Figures 12-16).

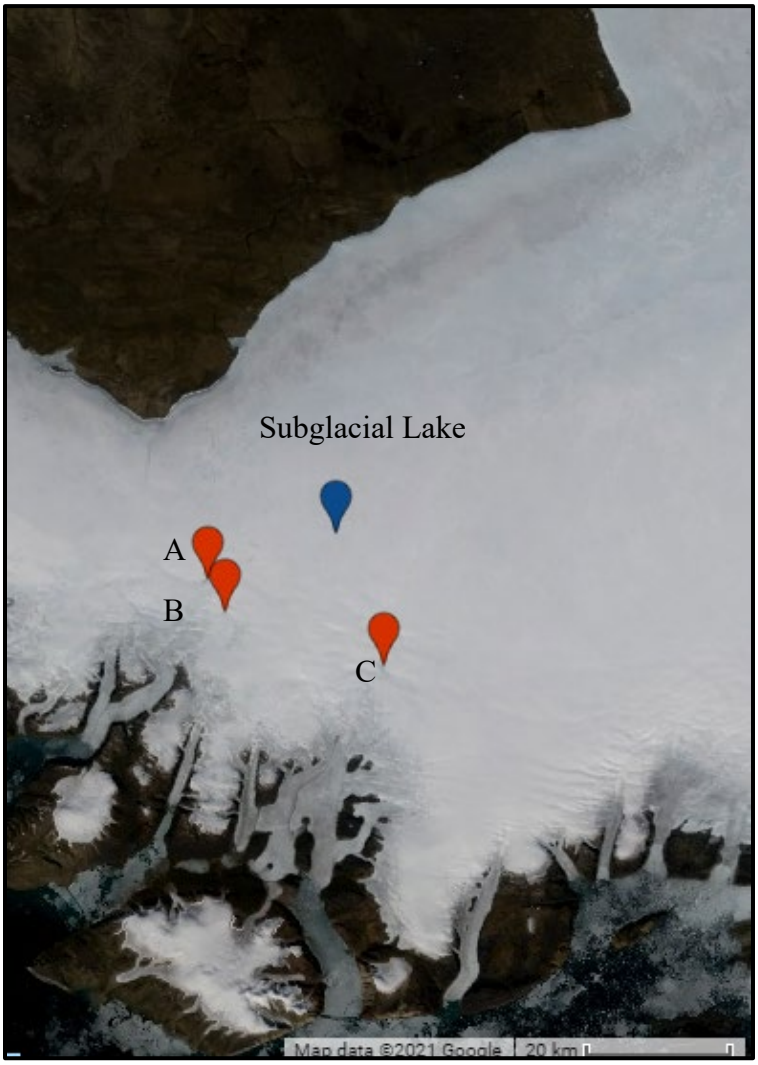

Figure 12: Subglacial and supraglacial lake locations from Landsat 8 imagery from the summer of 2015. Imagery from Google Earth

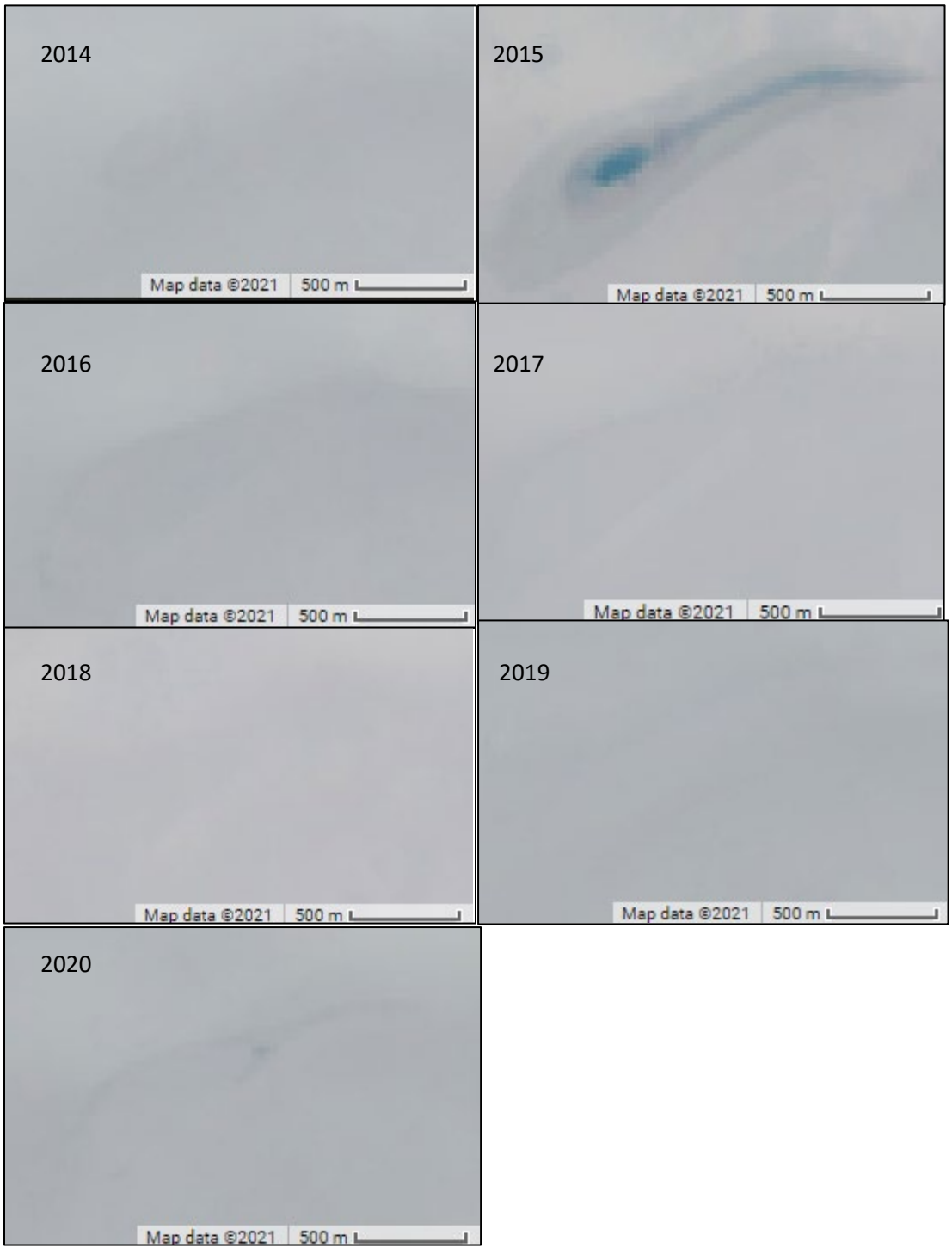

Figure 13: Landsat 8 Imagery of Lake A, located at 78.0426 N, 69.2307 W during June through August. 2015 was the only year where this lake contained mass liquid although it appears 2020 also had a small amount as well.

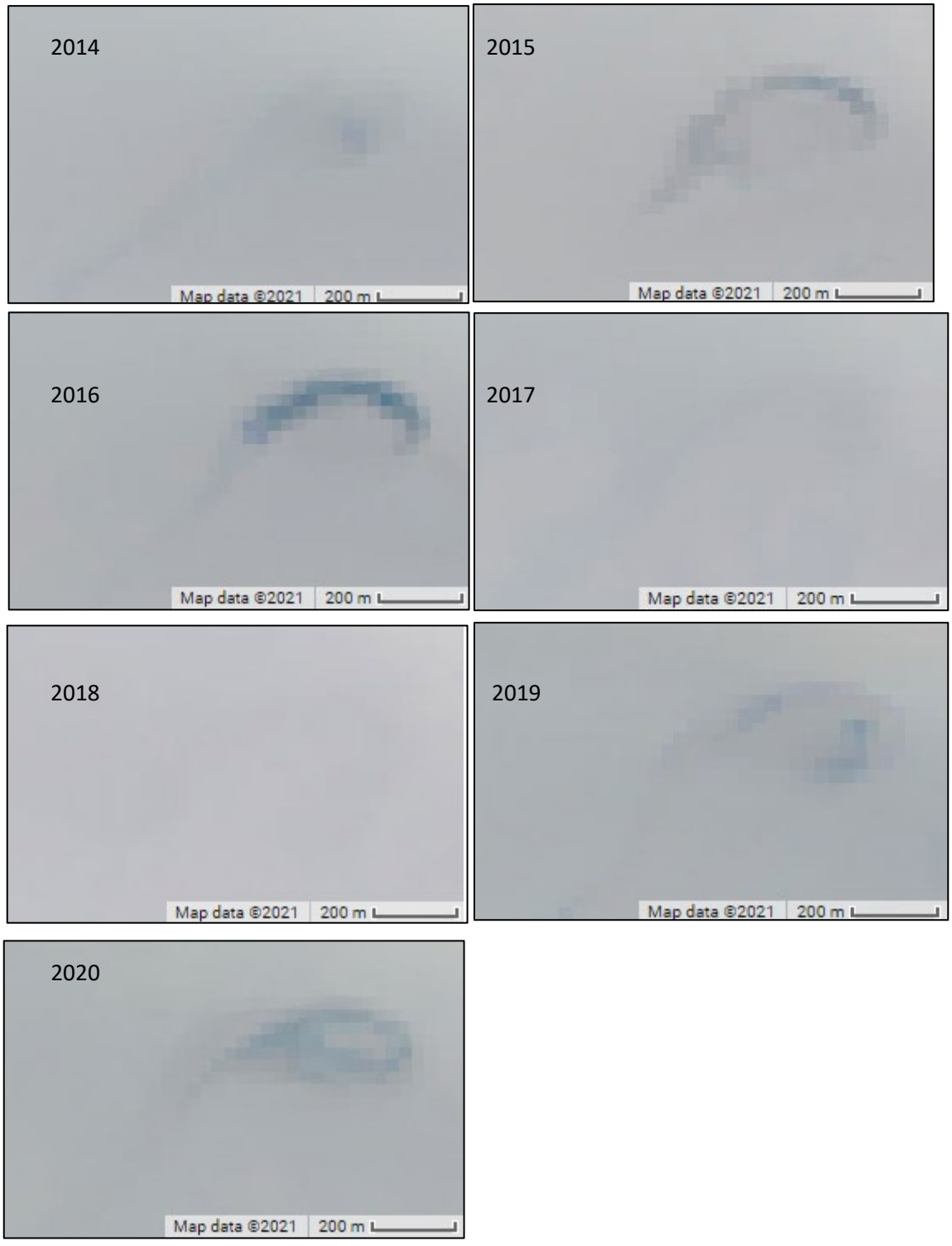

Figure 14: Landsat 8 imagery of Lake B, located at 78.0017 N,69.1382 W. Lake contains liquid in summers of 2015, 2016, 2019, and 2020, which are all years with higher average temperatures.

Figure 15: Landsat Imagery from Lake C, located at 77.9386 N, 68.2177 W. The lake is in a clear depression and, like lake A, has accumulated much meltwater in 2015 and some in 2020.

Figure 16: Landsat 8 Imagery of Subglacial Lake Coordinates. There are no major differences across the different summers at the surface.

From the appearance of the three supraglacial lakes, the most amount of meltwater by far was found in the summer of 2015. To further examine, imagery of the surrounding area of these three lakes were taken, shown in Figures 17 and 18.

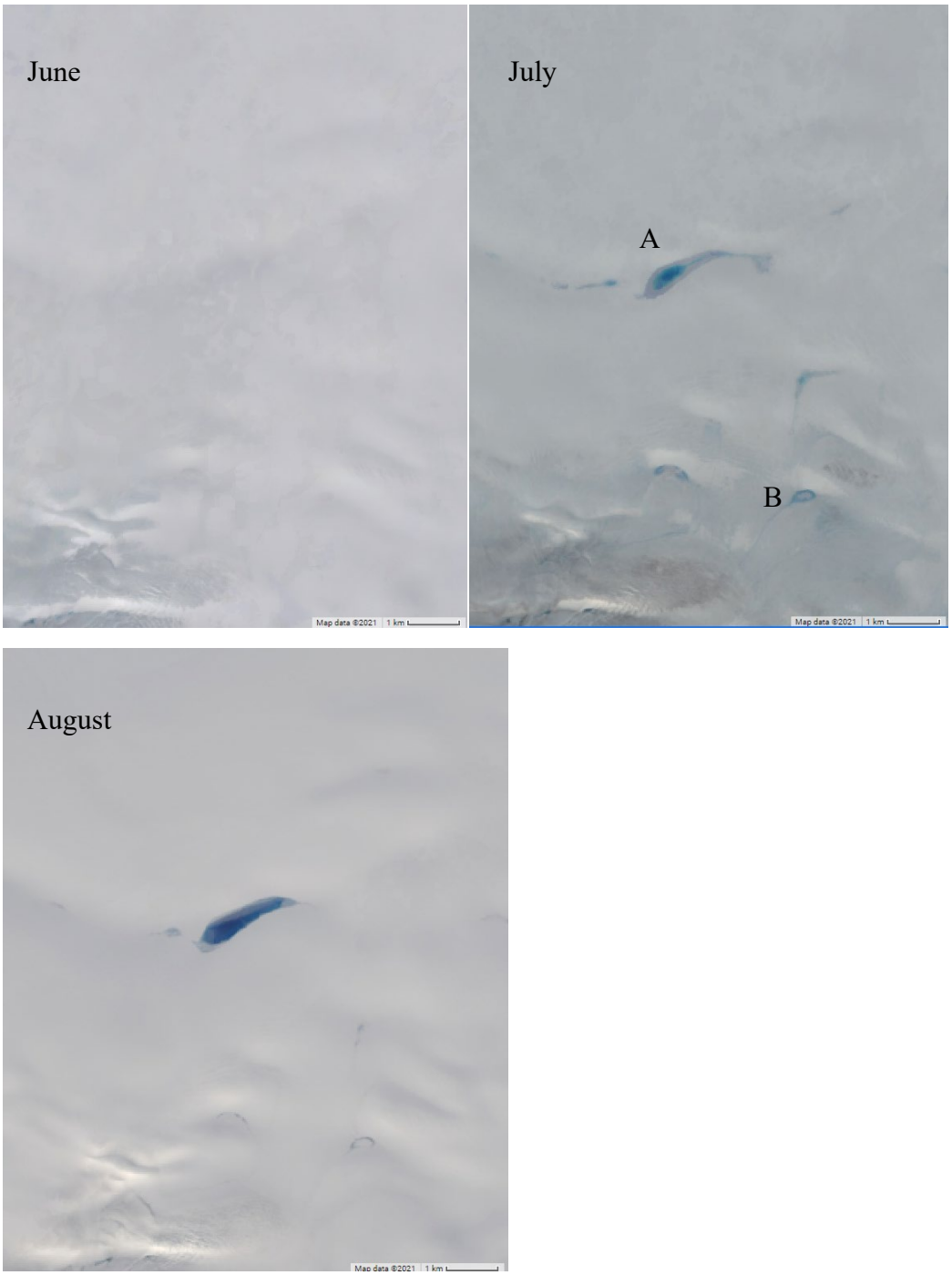

Figure 17: Landsat 8 imagery of Lake A and B during the summer season of 2015. There were additional lakes during July, the height of the melting season.

Figure 18: Landsat 8 imagery of Lake C during summer months of 2015. Similar to Lake A and B, there were additional supraglacial meltwater accumulation spots nearby.

Mass Loss

The first form of glacial changes that was explored was gravity/mass loss. Originally, it was nearly impossible to interpret the differences in mass loss between 2015 to other years. JPL's GRACE Data Analysis Tool provided data from the all the summer months in 2015, but 2014, 2016, 2017, and 2018 were all missing at least one summer month. In addition, the pixel sizes that NASA displays its data with were so large that it was impossible to determine the gravity loss between the different supraglacial lakes. The pixel sizes and GRACE measurements are shown in Figure 19 and 20. All gravity loss data is owned by NASA/JPL.

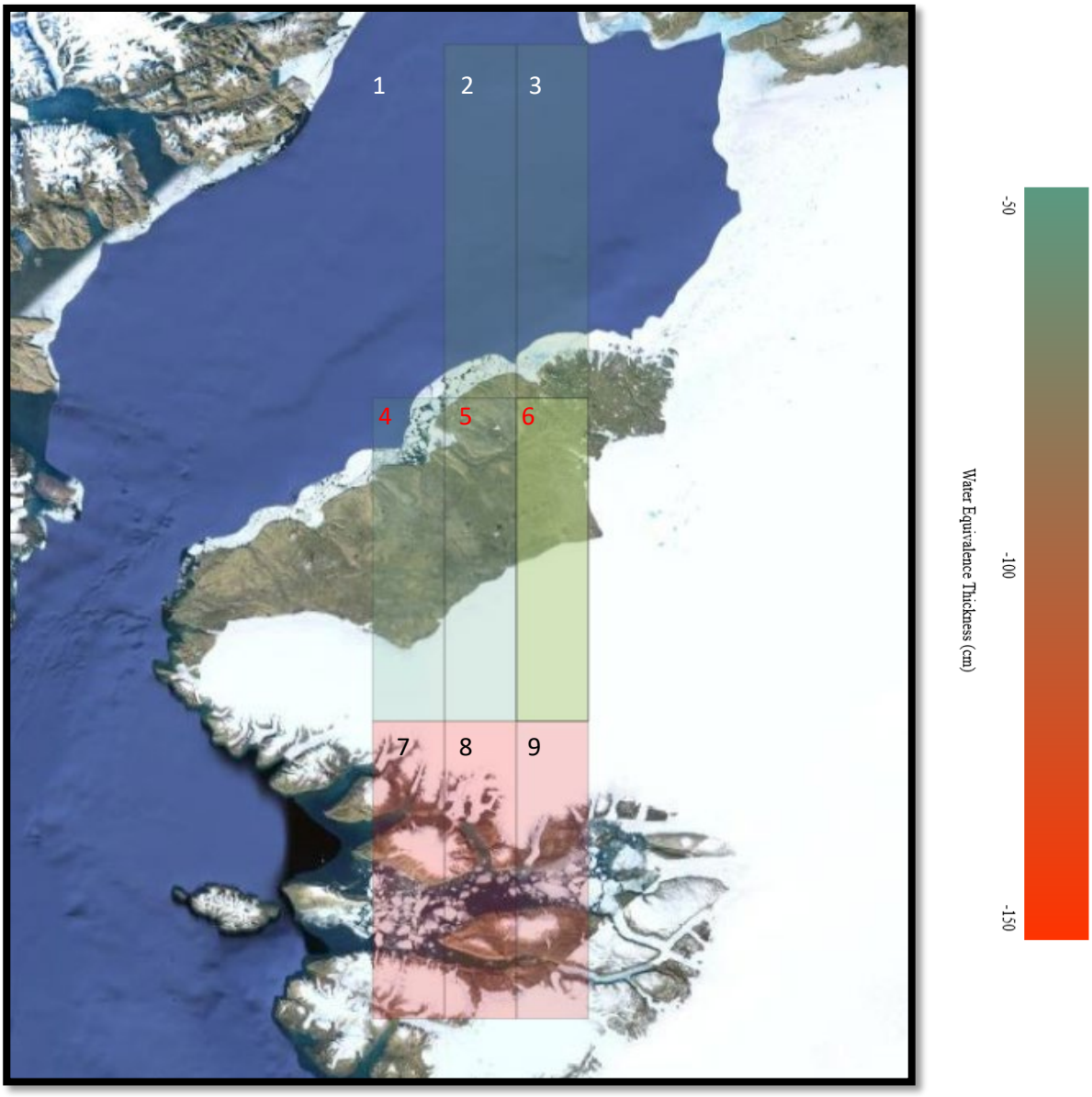

Figure 19: The Water Equivalent Thickness-Land provided by NASA were organized into a organized 3x3 grid. The subglacial lake is located at the border between pixels 5 and 8 and the supraglacial lakes are located in pixel 8. Basemap provided by ESRI and plotted using qGIS.

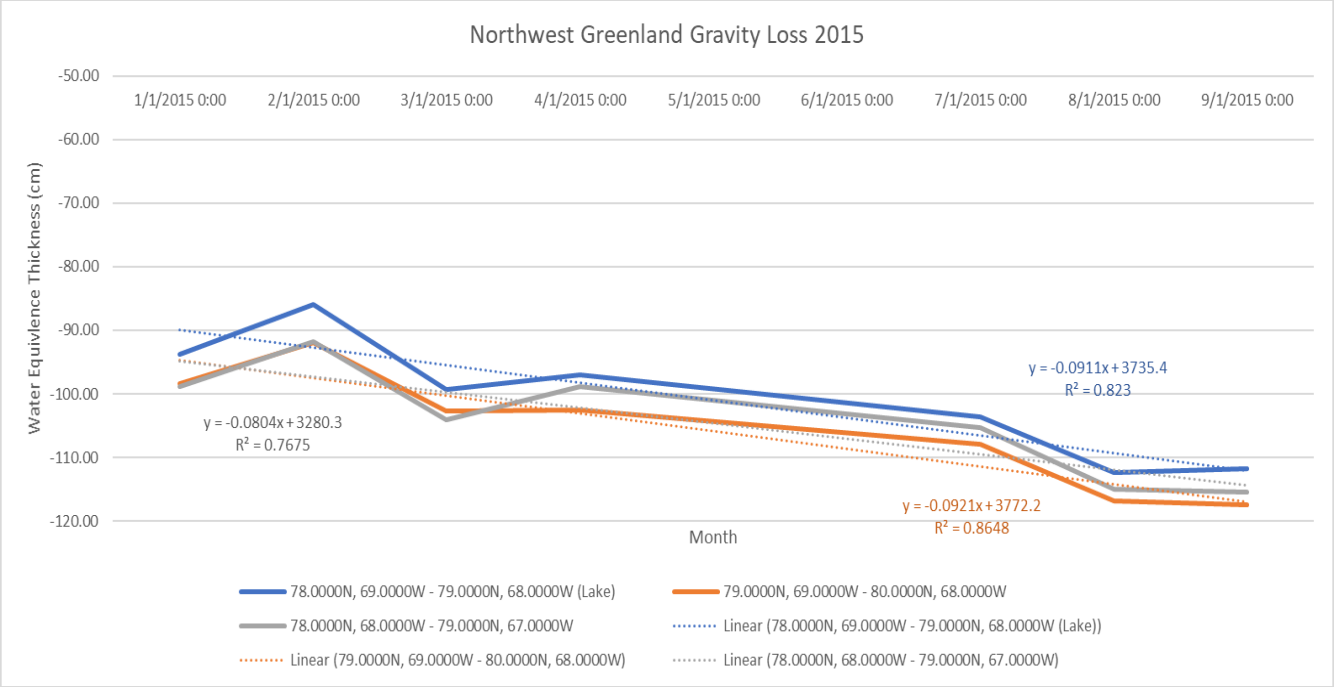

Figure 20: GRACE data from 2015, the year from which there was the most amount of meltwater accumulation.

GRACE data from the pixel 8 is missing data across all years. The original GRACE was shut down in 2018, hence the missing data. Follow-On (GRACE-FO) was initiated that same autumn, but the data following its inception showed consistency in all months. 2015, 2019 and 2020 are the only years with complete summer data. However, 2015 and 2019 were years with higher temperature ranges, and 2015 and 2020 had meltwater present in supraglacial lakes. The results of the six years are shown in Table 2 and Figures 21 and 22.

Table 2: Water Equivalent Thickness (cm)

Date	2014	2015	2016	2017	2019	2020
1-Apr	-198.71	-223.6	-266.34	-272.11	-294.12	-320.90
1-May	-200.74		-262.53	-279.84	-296.94	-317.95
1-Jun	-201.91	-246.91	-266.10	-278.53	-293.59	-320.32
1-Jul		-256.98	-275.37		-302.19	-335.43
1-Aug	-212.05	-257.99			-315.74	-346.91
1-Sep	-211.33				-320.44	-340.69
1-Oct	-211.39				-319.02	-336.98

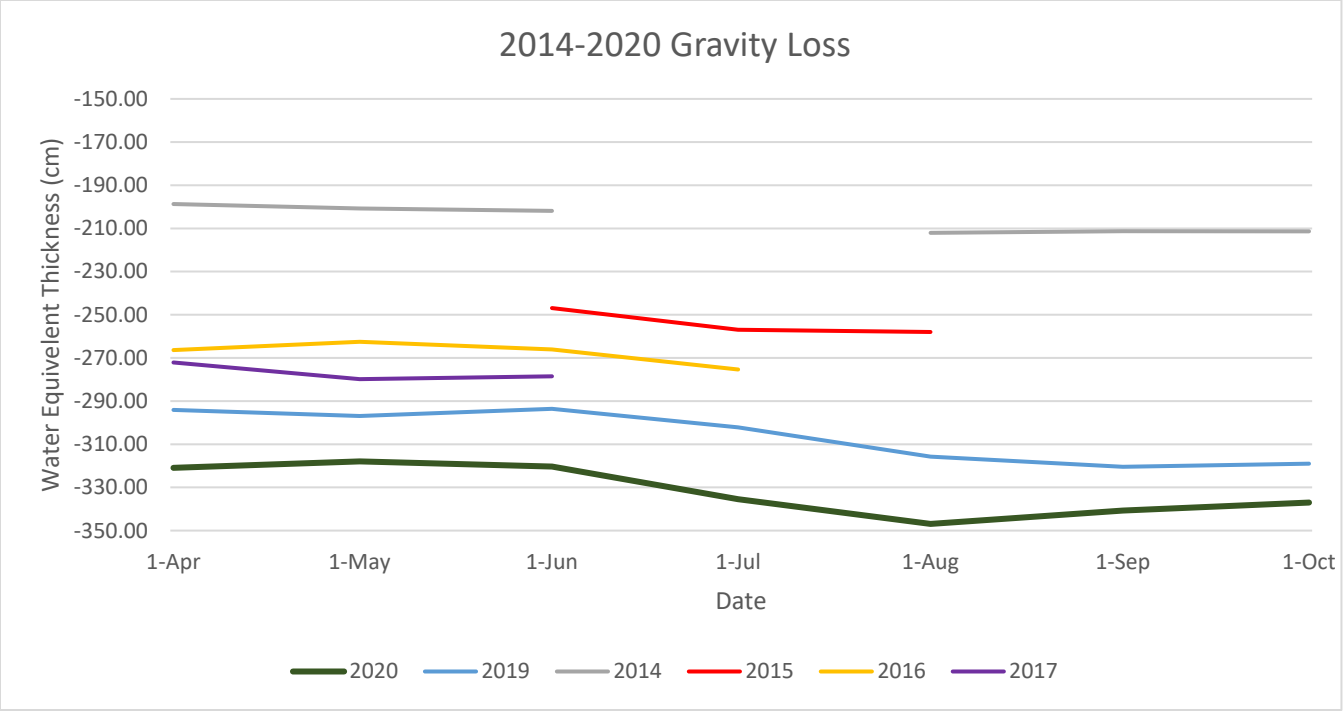

Figure 21: GRACE Data of pixel 8, excluding 2018.

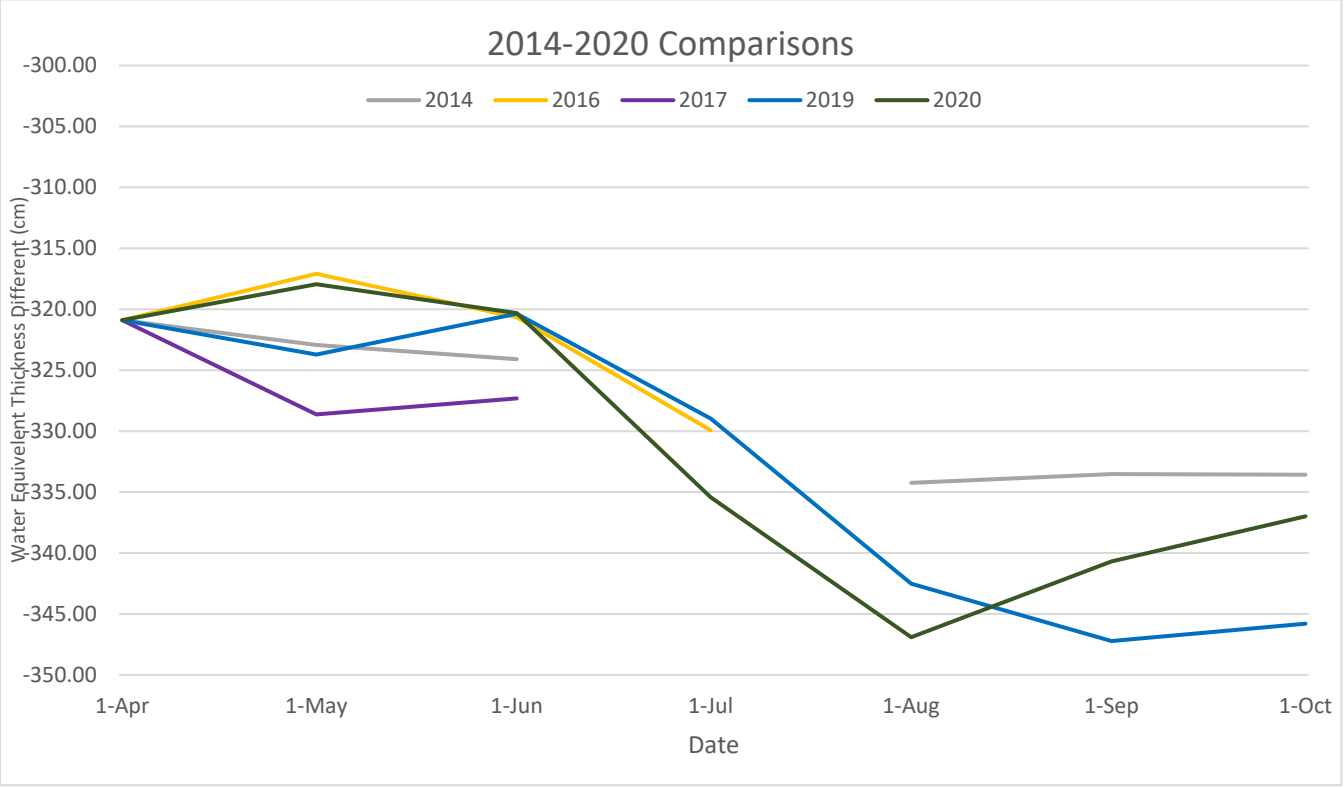

Figure 22: GRACE data values subtracted from the smallest value (2020) in April displaying the changes in gravity loss side by side.

The data from 2015 was missing values on April 1st, hence why it is not included on this graph. It is difficult compare different seasons as they sometimes change during spring and fall months. As stated earlier, 2015, 2019 and 2020 are the only years with all three summer months provided. Therefore, Figures 23 and 24 were made to reflect the mass loss in the summer/

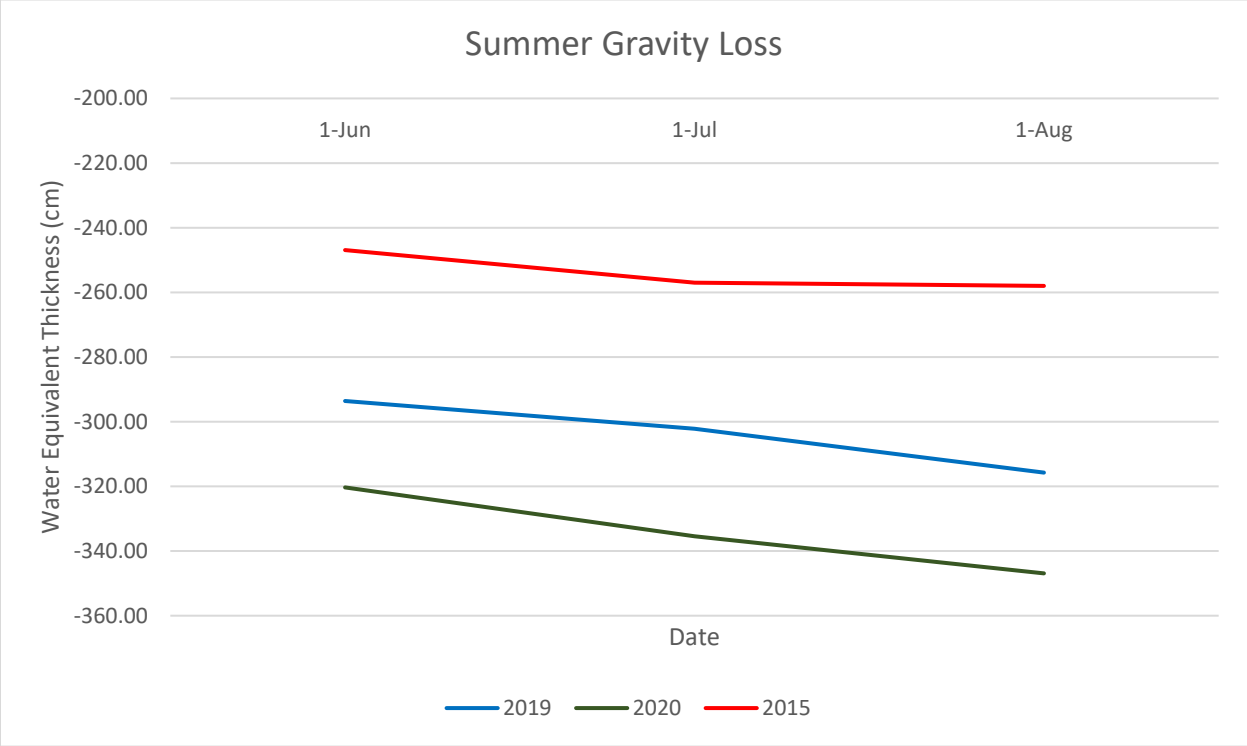

Figure 23: GRACE data for 2015, 2019 and 2020 summer months.

Figure 24: GRACE data values from Figure 23 were subtracted from the smallest value in June in order to compare linear slopes. Trendline equations are displayed on Tables 3 and 4.

Table 3: Equations for GRACE Trendlines

Year	Equation	Coefficient of Determination
2015	y = -0.1808x + 7697.4	0.8105
2019	y = -0.3636x + 15804	0.986
2020	y = -0.4355x + 18994	0.9923

However, 2015 had a significant difference in slope for June to July versus July to August.

Table 4: Two-Point Linear Equations for GRACE Data in 2015

Months	Equation
June-July	y = -0.3356x + 14564
July-August	y = -0.0326x + 1118.1

Even with considering the differences in slope for 2015, 2020 still had the greatest acceleration in negative Water Equivalent Thickness, which equates to greater mass loss. Even when considering just the mass loss in June alone, 2015 still experienced smaller mass loss in comparison to the other two years. From these data alone, the mass loss during the summer months did not appear to be correlated to the meltwater accumulation. However, GRACE calculated the WET values that cover a very large pixel including some much of the gulf to the south, which leads to possible errors in the results.

Ice Velocity

The next type of glacial flow measured was ice displacement. This was done using the National Ice and Snow Data Center's Greenland Ice Sheet Mapping Project's MEaSUREs Greenland Quarterly Ice Sheet Velocity Mosaics from SAR and Landsat, Version 2. This project combined satellite data from Synthetic Aperture Radar (SAR) from TerraSar-X/TanDEM-X and Senetinel-1A/1B. Using qGIS, the maps displaying ice displacement for years 2015-2018 were created. The hypotenuse, which would display the exact direction, was calculated from the X and Y data maps using a raster calculator. Unfortunately, 2020 is not available for public use yet. Figures 25-27 are the maps produced.

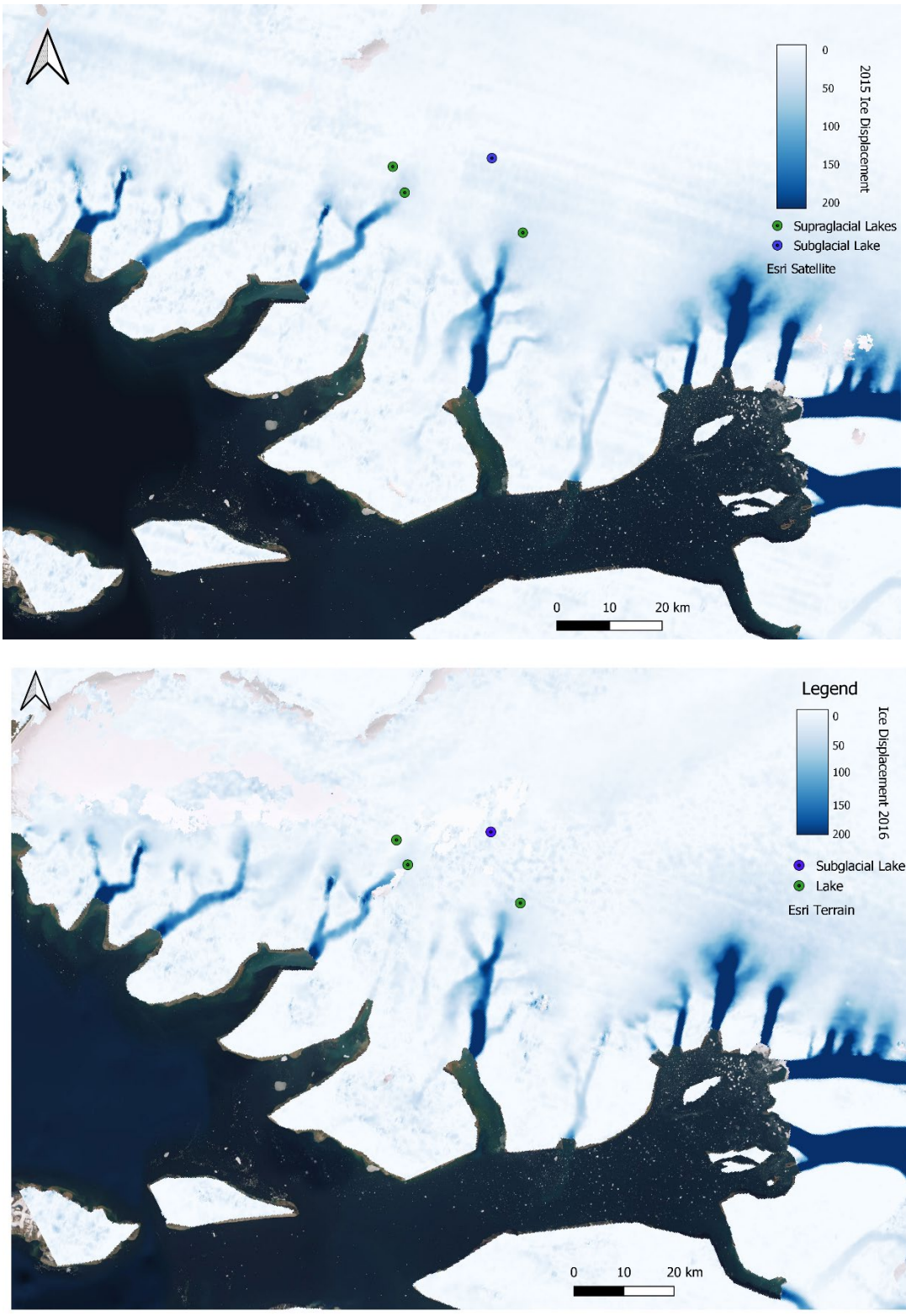

Figure 25: SAR Ice displacement ratio calculated for the summer of 2015 and 2016 for the region encompassing the supraglacial and subglacial lakes. Units are dimensionless. Map created using qGIS and Esri Satellite basemap (Joughin, 2020).

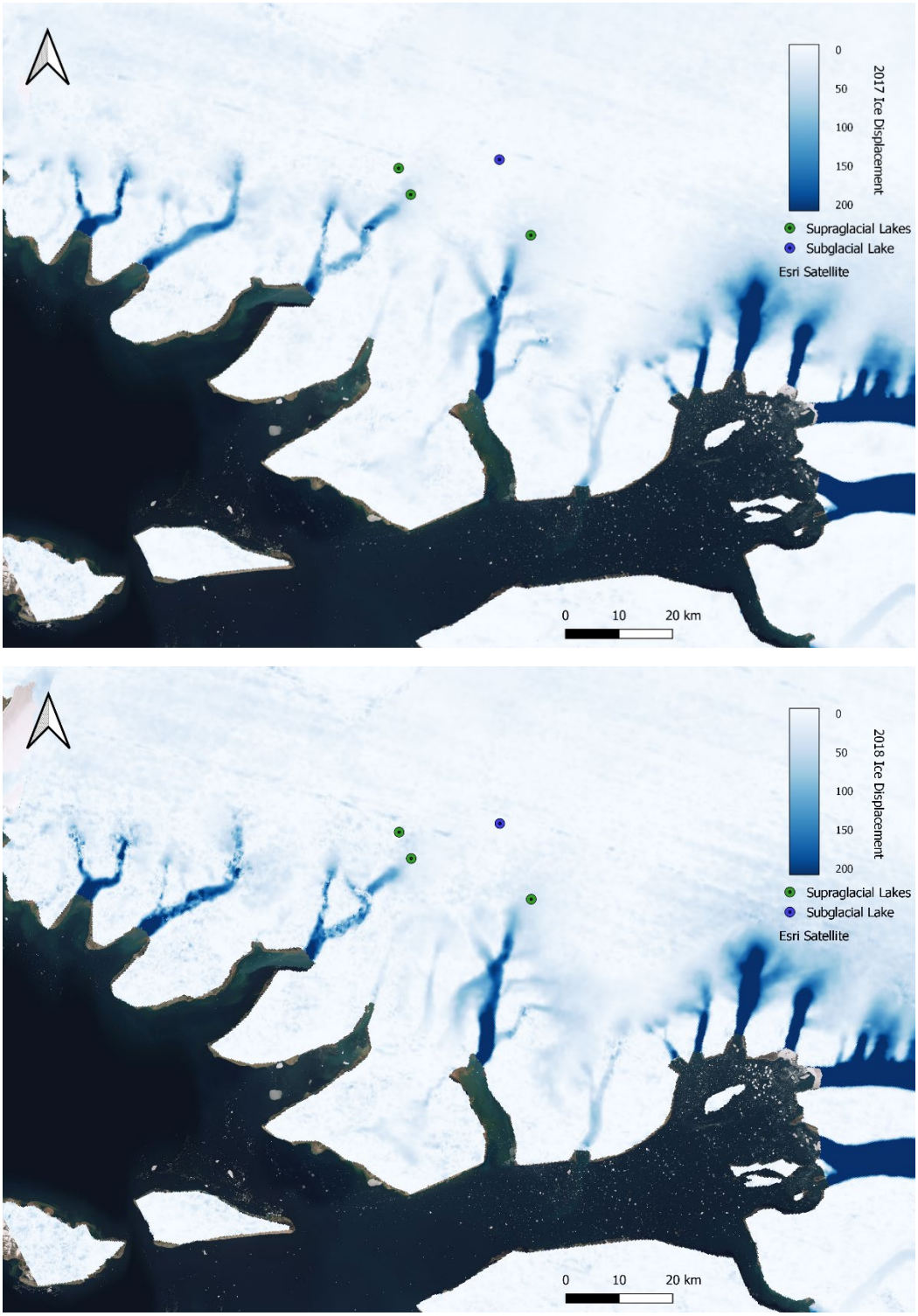

Figure 26: SAR Ice displacement ratio calculated for the summer of 2017 and 2018 for the region encompassing the supraglacial and subglacial lakes. Units are dimensionless. Map created using qGIS and Esri Satellite basemap (Joughin, 2020),

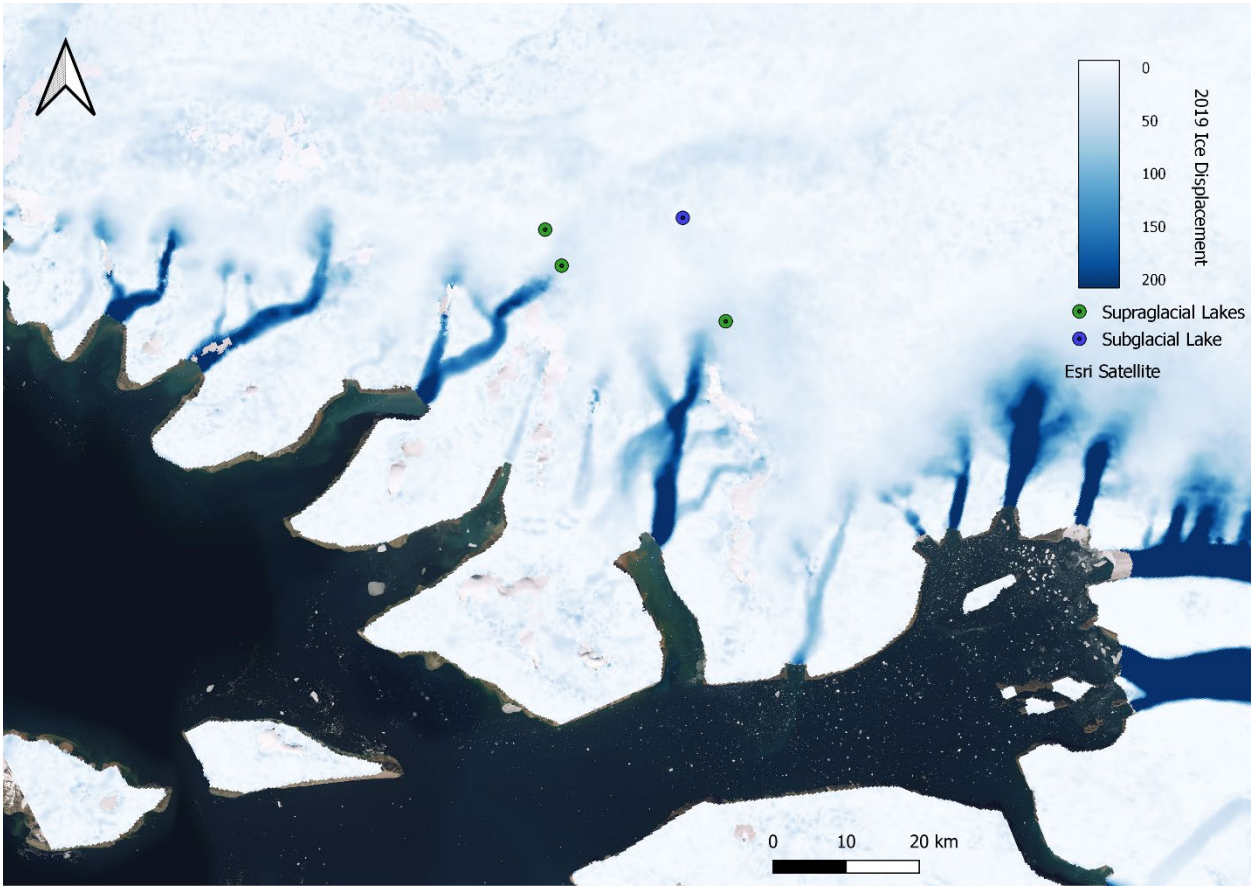

Figure 27: SAR Ice displacement ratio calculated for the summer of 2019 for the region encompassing the supraglacial and subglacial lakes. Units are dimensionless. Map created using qGIS and Esri Satellite basemap (Joughin, 2020).

As seen from the first four maps, there is hardly any difference of velocity on both the outlet glaciers and the ice sheet between 2015 and other years. The only year that has any noticeable difference is 2019, as the outlet glaciers demonstrate a smoother path in comparison to the other four years where the flow seem spotted. Even with a smaller scale, there was not any severe difference other than outlet flow position. Like mass loss, this does not indicate any correlation between ice velocity and meltwater accumulation, although it is difficult to make any decision without data from 2020.

Ice Thickness

Ice sheet thickness is the last glacial change that needs to be evaluated. Due to the presence of mass loss, much of the ice presumably has melted and discharged either through subglacial or supraglacial means. In addition, subglacial lake changes can result in small uplift (Willis et al., 2015). The European Space Agency Cryosat-2 satellite was launched in 2010. It is a polar altimeter satellite whose primary function is measuring the height of ice by measuring the altitude and echo over the surface at an interval of 50 microseconds (Zheng et al., 2018). For this project in particular, it was originally intended to retrieve the land-based thickness of the ice sheet in the study area. An ice baseline surface plot for the 2015 year was calculated using the MATLAB from NetCDF files (Fig 28 and 29).

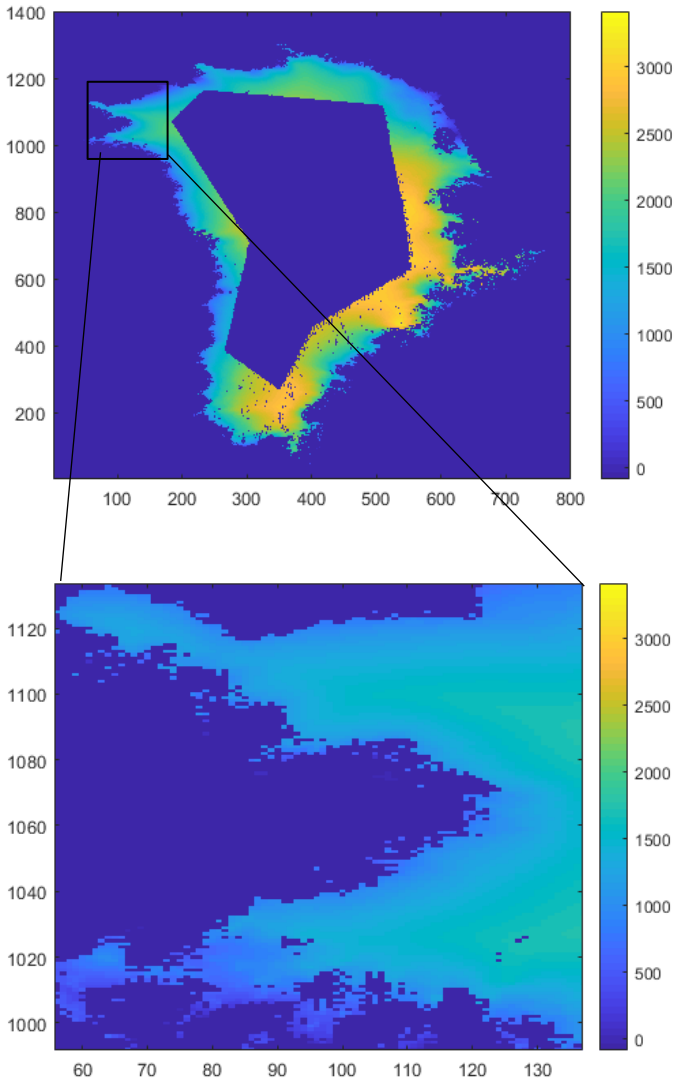

Figure 28: Ice Baseline-D Cryosat-2 Plot for June 2015, derived from NetCDF files using MATLAB. The northwest coast only shows ice thickness around 1000 to 1500 meters in comparison to the east coast where it can reach well over 3000 meters. ©ESA 2021

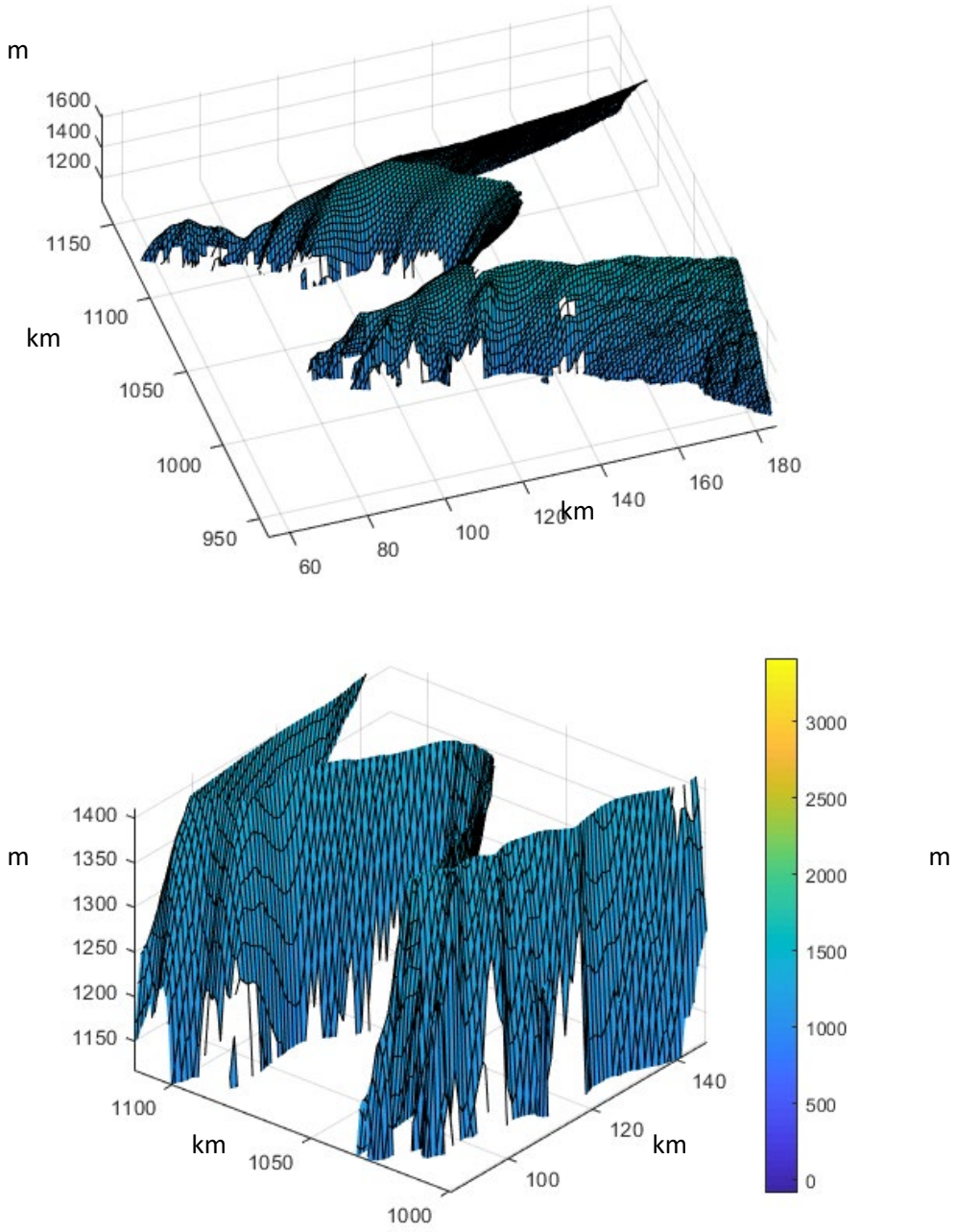

Figure 29: Ice Baseline-D Cryosat-2 Surface Plot for June 2015, derived from NetCDF files using MATLab. The coastal ice sheet starts at 1500 meters before sloping downwards rapidly. ©ESA 2021.

Unfortunately, the Ice Baseline-D files that were used earlier in February were unexpectantly replaced with double files for the 2016-2018 year while GRACE data was being revisited. Along with this, the NetCDF files that remained public did not have a proper "elevation" or Z-vector, preventing production of a surface plot. Attempts to replicate the data into new matrices or raster files did not produce proper plots. Unfortunately, the changes in ice elevation are not available for current analysis during the time frame and are not usable in this project any longer.

Conclusion

The number and size of supraglacial lakes in northwest Greenland increased in 2015. Despite the amount of meltwater accumulation being much higher in 2015, it had roughly the same amount of mass loss as 2019 during the month of June, and about 77% of the amount of mass loss during 2020. Meanwhile, the ice displacement for the years 2015-2018 were roughly the same despite differences in air temperature. From displacement and mass loss, there was no direct correlation between any of the changes in glacial movement to the formation of supraglacial lakes near the subglacial lake in Northwest Greenland during the peak year of 2015. The reason why 2015 had such a large amount of meltwater accumulation is unknown at this point. A possible reason is the number and volume of debris and/or dark spots that could decrease albedo and increase melting rates in those areas. To do so would require studies using radiation detecting equipment such as Clouds and Earth Radiant Energy System (Smith et al., 2011). In addition, there are theories that the bulk of supraglacial lakes are being observed further inland as they typically form near the ablation zones (hence why the three lakes are close to the coast) (Leeson et al., 2014). This might explain why there has been a lack of resurgence in the observed lakes. Possible future research might try to expand the study area further inland. Since new subglacial lakes are still being discovered, future nearby lakes could also be analyzed. However, the correlation between the changes in mass loss/ice displacement and meltwater accumulation is not apparent on the northwest coast.

Bibliography

Acharya, T., Yang, I. (2015). Exploring Landsat 8. International Journal of IT, Engineering and Applied Sciences Research. 4, 4, 4-10.

Acker, J.G., &. Leptoukh, G. (2007). Online Analysis Enhances Use of NASA Earth Science Data, Eos, Trans. *AGU*. 88, 2, 14 & 17.

Bowling, J.S., Livingtone, S.J., Sole. A.K., Chu W. (2019). Distribution and dynamics of Greenland subglacial lakes. *Nature Communications*. 10, 2810. https://doi.org/10.1038/s41467-019-10821-w

Featherstone, W.E., Dentith M.C. (1997). A geodetic approach to gravity data reduction for geophysics. *Computers & Geosciences*. 23, 10, 1063-1070. https://doi.org/10.1016/S0098-3004(97)00092-7

Hackney, R.I., Feathersone, W.E. (2003). Geodetic versus geophysical perspectives of the 'gravity anomaly'. *Geophysical Journal International.* 154, 1, 35-43

Howat, I.M., Porter, C., Noh, M.J., Smith, B.E., Jeong, S. (2015). Brief Communication: Sudden drainage of a subglacial lake beneath the Greenland Ice Sheet. *The Cryosphere*. 9, 103-108. https://doi.org/10.5194/tc-9-103-2015

Jeffries, M.O., Richter-Menge, J., & Overland, J.E. (2015). Arctic Report Card 2015, https://www.arctic.noaa.gov/Portals/7/ArcticReportCard/Documents/ArcticReportCard_full_report2015.pdf

Jiang, D., Wang, J., Huang, Y., Zhou, K., et al. (2014). The Review of GRACE Data Applications in Terrestrial Hydrology Monitoring. *Advances in Meteorology*. 2014. https://doi.org/10.1155/2014/725131

Joughin, I. (2020). MEaSUREs Greenland Quarterly Ice Sheet Velocity Mosaics from SAR and Landsat, Version 2. Boulder, Colorado USA. NASA National Snow and Ice Data Center Distributed Active Archive Center. https://doi.org/10.5067/3ZMCUIFDYJG4.

Leeson, A.A., Shpherd, A., Briggs, K., Howat, I., et al. (2014). Supraglacial lakes on the Greenland ice sheet advance inland under warming climate. *Nature Climate Change*. 5, 51-55. https://doi.org/10.1038/nclimate2463

Moy, E. (2019). In-situ GPS Measurement of the Ice Flow Velocity Near an Ice Divide Overlying a Subglacial Lake in Northwestern Greenland. *Undergraduate Senior Thesis, University of Maryland GEOL 394.*

NASA Facts. (2003). Studying the Earth's Gravity from Space: The Gravity Recovery and Climate Experiment (GRACE). grace.jpl.nasa.gov/system/internal_resources/details/original/97_GRACE_Fact_Sheet.pdf

Lüthje, M., Pedersen, L., Reeh, N., & Greuell, W. (2006). Modelling the evolution of supraglacial lakes on the West Greenland ice-sheet margin. *Journal of Glaciology*, 52, 179, 608-618. doi:10.3189/172756506781828386

Osborne, E., Richter-Menge, J., Jeffries, M. (2018). Arctic Report Card 2018. https://arctic.noaa.gov/Portals/7/ArcticReportCard/Documents/ArcticReportCard_full_report2018.pdf

Palmer, S., McMillan, M., Morlighem, M. (2015). Subglacial lake drainage detected beneath the Greenland ice sheet. *Nature Communications*. 6, 8408. https://doi.org/10.1038/ncomms9408

Reis, J., Bettadpur, S., Eanes, R., Kang, Z., et al. (2016). Development and Evaluation of the Global Gravity Model GGM05, CSR-16-02. Center for Space Research, the University of Texas at Austin.

Ritcher-Menge, J., Druckenmiller, M.L., & Jeffries, M. (2019). Arctic Report Card 2019. https://www.arctic.noaa.gov/Portals/7/ArcticReportCard/Documents/ArcticReportCard_full_report2019.pdf

Ritcher-Menge, J., Overland, J.E., & Mathis, J.T. (2016). Arctic Report Card 2016. https://www.arctic.noaa.gov/Portals/7/ArcticReportCard/Documents/ArcticReportCard_full_report2016.pdf

Ritcher-Menge, J., Overland, J.E., Mathis, J.T, & Osborne, E. (2017). Arctic Report Card 2017. https://arctic.noaa.gov/Portals/7/ArcticReportCard/Documents/ArcticReportCard_full_report2017.pdf

Smith, G.L., Priestley, K.K., Loeb, N.G., Wielicki, B.A., et al. (2011). Clouds and Earth Radiant Energy System (CERES), a review: Past, present and future. *Advances in Space Research*. 48, 2, 254-263. https://doi.org/10.1016/j.asr.2011.03.009

Sundal, A.V., Shepherd, A., Niewnow, P., Hanna, E., et al. (2009). Evolution of supra-glacial lakes across the Greenland Ice Sheet. *Remote Sensing of Environment.* 113, 10, 2164-2171. https://doi.org/10.1016/j.rse.2009.05.018

Thoman, R.L., Richter-Menge, J., & Druckenmiller, M. (2020). Arctic Report Card 2020. https://doi.org/10.25923/mn5p-t549

Velicogna, I., Sutterley, T.C., van den Broeke, M.R. (2014). Regional acceleration in ice mass loss from Greenland and Antarctica using GRACE time-variable gravity data. *Geophysical Research Letters.* 41, 22, 8130-8137. https://doi.org/10.1002/2014GL061052

Willis, M., Herried, B., Bevis, M., Bell, R. (2015). Recharge of a subglacial lake by surface meltwater in northeast Greenland. *Nature*. 518, 223–227. https://doi.org/10.1038/nature14116

Zheng, Q., Klemas, V.V., Yan, X.H. (2018). 8.01 - Volume 8 Overview: Progress in Ocean Remote Sensing. *Comprehensive Remote Sensing.* 8, 1-42.

Appendix:

Landsat 8 Reflectance Python Code, processed in Google Earth Engine.

```
function maskL8sr(image) {
  // Bits 3 and 5 are cloud shadow and cloud, respectively.
  var cloudShadowBitMask = (1 << 3);
  var cloudsBitMask = (1 << 5);
  // Get the pixel QA band.
  var qa = image.select('pixel_qa');
  // Both flags should be set to zero, indicating clear conditions.
  var mask = qa.bitwiseAnd(cloudShadowBitMask).eq(0)
                 .and(qa.bitwiseAnd(cloudsBitMask).eq(0));
  return image.updateMask(mask);
}

var dataset2015 = ee.ImageCollection('LANDSAT/LC08/C01/T1_SR')
                  .filterDate('2015-06-01', '2015-8-31')
                  .map(maskL8sr);
var dataset2014 = ee.ImageCollection('LANDSAT/LC08/C01/T1_SR')
                  .filterDate('2014-06-01', '2014-8-31')
                  .map(maskL8sr);
var dataset2016 = ee.ImageCollection('LANDSAT/LC08/C01/T1_SR')
                  .filterDate('2016-06-01', '2016-8-31')
                  .map(maskL8sr);
var dataset2017 = ee.ImageCollection('LANDSAT/LC08/C01/T1_SR')
                  .filterDate('2017-06-01', '2017-8-31')
                  .map(maskL8sr);
var dataset2018 = ee.ImageCollection('LANDSAT/LC08/C01/T1_SR')
                  .filterDate('2018-06-01', '2018-8-31')
                  .map(maskL8sr);
var dataset2019 = ee.ImageCollection('LANDSAT/LC08/C01/T1_SR')
                  .filterDate('2019-06-01', '2019-8-31')
                  .map(maskL8sr);
var dataset2020 = ee.ImageCollection('LANDSAT/LC08/C01/T1_SR')
                  .filterDate('2020-06-01', '2020-8-31')
                  .map(maskL8sr);
var visParams = {
  bands: ['B4', 'B3', 'B2'],
  min: 500,
  max: 15000,
  gamma: 1.4,
};
Map.setCenter(-68.467, 78.0574, 8);
Map.addLayer(dataset2015.median(), visParams,'2015');
Map.addLayer(dataset2014.median(), visParams,'2014');
```

```
Map.addLayer(dataset2016.median(), visParams,'2016');
Map.addLayer(dataset2017.median(), visParams,'2017');
Map.addLayer(dataset2018.median(), visParams,'2018');
Map.addLayer(dataset2019.median(), visParams,'2019');
Map.addLayer(dataset2020.median(), visParams,'2020');
Export.image.toDrive({
  image: dataset2015.median(),
  description: 'Collasped Basin 2015',
  scale: 10,
  fileFormat: 'GeoTIFF',
  region: AOI
});
Export.image.toDrive({
  image: dataset2014.median(),
  description: 'Supraglacial 2015',
  scale: 10,
  fileFormat: 'GeoTIFF',
  region: supraglacial1
});
```

Acknowledgments

I acknowledge the MODIS mission scientists and associated NASA personnel for the production of the data used in the research from Giovanni.

I acknowledge the full title and ownership, including all derived rights, by ESA of all ESA data.

I pledge on my honor that I have not given or received any unauthorized assistance or plagiarized on this assignment.

Kendal Grubb